TAMPEREEN TEKNILLINEN YLIOPISTO
TAMPERE UNIVERSITY OF TECHNOLOGY

ARMAN DASTPAK

DEVELOPMENT AND CHARACTERIZATION OF CARBON-BASED ELECTRODE MATERIALS AND THEIR IMPLEMENTATION IN SUPERCAPACITORS

Master of Science thesis

Examiners:
Prof. Donald Lupo
Prof. Jyrki Vuorinen
Project Manager Jari Keskinen
Faculty Council of the Faculty of Engineering Sciences
on 4th November 2015

ABSTRACT

Arman Dastpak: Development and characterization of carbon-based electrode materials and their implementation in supercapacitors
Tampere University of Technology
Master of Science Thesis, 54 pages
December 2015
Master's Degree Programme in Materials Science
Major: Materials Research
Examiner: Prof. Donald Lupo, Prof. Jyrki Vuorinen, Project manager Jari Keskinen

Keywords: Carbon electrodes, Aqueous-based supercapacitors, flexible printable electronics, EDLC

Supercapacitors are energy storage devices, in which storage of energy is based on the formation of electric double layer at the interface of electrode and electrolyte. In general, a porous structure of electrode is needed to increase the surface area for formation of the electric double layer.

The focus of this work was to design flexible supercapacitors, based on printing of different carbon-based inks. Three classes of materials were tested: activated carbon (AC), graphene, and carbon nanotubes (CNT). A precondition of the work was to use environmentally friendly aqueous electrolyte. A problem arising from the use of aqueous based electrolytes is the corrosion of current collectors. Therefore, the aim was to eliminate the corrosion of metallic current collector. This was done by changing the supercapacitor structure. The electrodes were fabricated on flexible polyethylene terephthalate (PET)-based substrates by blade coating.

The supercapacitors were electrically characterized using the IEC 62391-1 international standard. From the galvanostatic charge-discharge measurement, capacitance values and equivalent series resistance (ESR) were measured. In addition, cyclic voltammetry (CV) was utilized to study the general behavior of supercapacitors. Moreover, the specific surface area (SSA) of electrodes was obtained from Brunauer, Emmett, and Teller (BET) method.

The highest specific capacitance was obtained from activated carbon electrodes with values of 33 F/g. The SSA of AC was 1741 m^2/g, which indicates that AC electrode material compromise a high concentration of pores. The specific capacitance obtained from CNTs was small, with the highest value of 5 F/g. Therefore, further development of CNT inks is necessary in order to make them a successful candidate as the electrode of printable supercapacitors. Moreover, ESR was primarily minimized by a suitable combination of electrode and current collector taking account of the corrosion risk caused by aqueous electrolyte.

PREFACE

This work was carried out at Tampere University of Technology with direct funding of TUT in support of the Tekes FiDiPro project PAUL. The work was done at the department of Electronics and Communication.

I would like to thank my supervisor Prof. Donald Lupo for giving me this opportunity to be part of his research group, as well as his guidance and advices during the process. I am also grateful for the counseling I received from my examiner Prof. Jyrki Vuorinen. I also wish to thank Jari Keskinen for helping me to have a better understanding of both practical and theoretical aspects of this work. I would like to express my gratitude to Suvi Lehtimäki for her useful advice during this project.

This work is dedicated to my family, especially my mother for her endless kindness and support. At the end, I am grateful for the support and motivation I have received from my friends Vala, Masoud, Armin, and Shadi.

Tampere, December 2015

Arman Dastpak

CONTENTS

LIST OF FIGURES

LIST OF SYMBOLS AND ABBREVIATIONS

AC	Activated carbon
BET	Bruanauer, Emmett, Teller. An analysis method for surface area measurements
CNT	Carbon nanotube
CV	Cyclic voltammetry
CVD	Chemical vapor deposition
DLG	Double layer graphene
DWNT	Double wall nanotube
EDL	Electrical double layer
EET	Electrochemical energy storage
ESR	Equivalent series resistance
FLG	Few layer graphene
H_2O_2	Hydrogen peroxide
HCl	Hydrochloric acid
IHP	Inner Helmholtz plane
MnO	Manganese oxide
MWNT	Multiwall nanotube
NaCl	Sodium chloride
NiO	Nickel oxide
OHP	Outer Helmholtz plane
PE	Polyethylene
PET	Polyethylene terephthalate
RuO	Ruthenium oxide
SC	Supercapacitor
SLG	Single layer graphene
SSA	Specific surface area
SWNT	Single wall nanotube
TEM	Transmission electron microscopy
ΔU_3	IR drop
ε_0	Dielectric constant in vaccum
ε_r	Dielectric constant in electrolyte
A	Specific surface area
C	Capacitance
d	Thickness of electric double layer
d_v/d_t	Voltage sweep rate
E	Maximum stored energy
G	Geometry correction factor
I	Current
K	Kelvin
P	Power
P_0	Maximum power
R_L	Load resistance
R_S	Equivalent series resistance
U	Maximum system voltage

U_1	Voltage at 80% of maximum voltage in galavanostatic measurements
U_2	Voltage at 40% of maximum voltage in galavanostatic measurements
U_R	Maximum voltage of system in galavanostatic measurements

1. INTRODUCTION

The adverse impact of fossil fuels on the environment and human health has led to a growing demand for renewable energy sources and new technologies for electrical energy storage systems. Moreover, development of stationary and mobile systems has increased the need of storage systems with ability to deliver high power and energy densities [1][2]. Although batteries can provide high energy densities, their low power density and poor cycle life limits their use in applications requiring high power-and many change cycles [3]. Supercapacitors received a great deal of attention because of their unique combination of properties such as high power densities, long cycle life, and high energy efficiencies [1]. These devices are particularly suitable for applications which require energy pulses in short periods of time [3].

Printed electronics is an emerging field with a huge potential in large-scale production of flexible electronic devices with low cost [4]. The fast development of new generations of thin, flexible, and cheap electronics has increased the need for new methods of production such as roll-to-roll printing. The emerging field of "printed electronics" includes printable transistors, solar cell, organic diodes, as well as charge storage devices. Printable electronics can enable the low cost and fully-integrated manufacturing of electronic devices [5].

Currently available commercial supercapacitors are mainly based on the use of high surface area porous carbon materials or metal oxide systems [6]. Carbon-based materials are mainly used because of their low cost, easy process ability, controllable porosity, and various natural forms [7]. However, development of supercapacitors is still ongoing, and they require improvement especially in their energy density values. Therefore, for improvement of these devices a fundamental understanding materials, properties, and operating principles is necessary [3].

The theoretical part of thesis introduces the main parameters, which determine the performance of printed electrodes in a supercapacitor. The experimental part reports the testing of the performance of different carbon-based inks as electrodes of supercapacitors. Finally, three different supercapacitor architectures with various current collector designs were fabricated and characterized to study the effect on performance of both the electrode material and current collector design.

2. PRINCIPLE OF SUPERCAPACITORS

A supercapacitor (SC, also known as electrochemical capacitor or electric double layer capacitor) is an electrochemical energy storage (EES) system, in which accumulation of charged particles leads to storage of energy [8][9]. In contrast to other dominant EES systems such as batteries and fuel cells, in supercapacitors the storage of energy takes place at the electrode/electrolyte interface. In general, the performance of supercapacitors has been evaluated by measuring various parameters such as energy density (energy stored per unit weight/volume), power density (W kg^{-1} or W L^{-1}), and specific capacitance (F g^{-1}) [10]. In terms of electrical properties, supercapacitors take place between conventional capacitors and batteries. Batteries are typically low power devices, whereas conventional capacitors may have a high power density values at very low energy density. Electrochemical capacitors have an improved performance, in terms of power density, in comparison to batteries. In addition, electrochemical capacitors are expected to have a much longer cycle life than batteries because no or negligibly small chemical charge transfer reactions are involved [9].

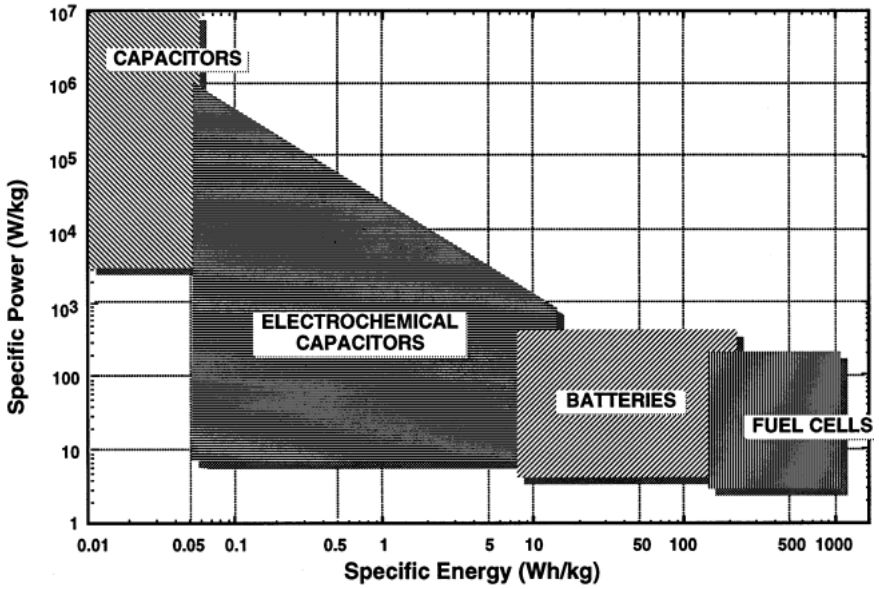

Figure 1. *Comparison of the specific energy/power density values for different energy storage systems* [9].

In general, there are two main differences between batteries and supercapacitors; their charge storage mechanisms and dissimilarities in their materials/structures. In terms of energy density, batteries are designed to provide high values by storing charge in bulk electrodes. On the other hand, energy density values for supercapacitors are limited to

values of 5-10 Wh kg^{-1}, compared to 100~250 Wh kg^{-1} for Li-ion batteries. However, batteries suffer from various limitations such as short cycle life, and slow charge/discharge rates. In contrast to batteries, high power density values can be achieved using supercapacitors (1-2 orders of magnitude higher than that of batteries). Therefore, storage and release of energy in supercapacitors can occur in the time frame seconds or less, in comparison to tens of minutes or more for batteries. Furthermore, the cycle life of supercapacitors is typically 2-3 orders of magnitude higher than the cycle life of batteries [10].

Supercapacitors consist of two conductive electrodes and two current collectors, which are separated from each other by a layer that does not allow electron conductivity but does allow ions to pass through it. Moreover, there is an electrolyte solution between electrodes, in which conduction of ions occurs [11] (see section 2.2). A schematic illustration of this system can be seen in figure 2. The energy storage process of SC is based on the accumulation and separation of electrical charge. The charge accumulation occurs in the electrochemical double layer at the electrode/electrolyte interface. In other words, applying a voltage potential across the system leads to movement of charged ions, and during the process negative ions in the electrolytes will be transferred to the positive electrode. It is also the case for positive ions, which will be transferred to the negative electrodes [7].

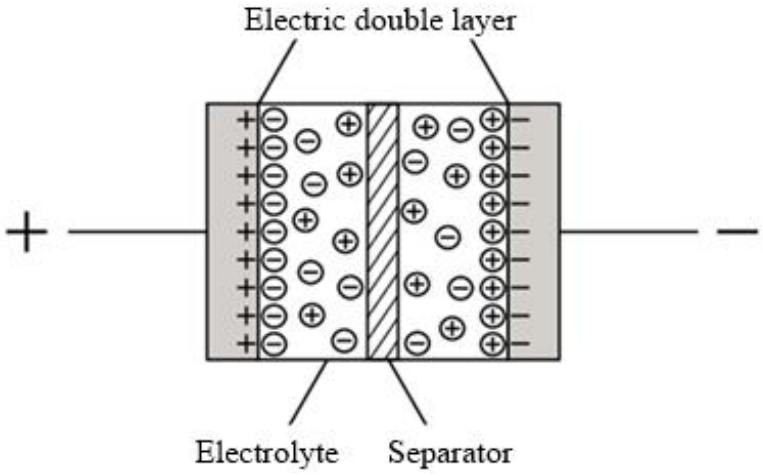

Figure 2. *Structure of supercapacitors [5]*.

The capacitance values (C) for capacitors can be described according to equation 1:

$$C = \frac{\varepsilon_0 \varepsilon_r A}{d}, \qquad \textbf{\textit{Equation 1}}$$

where A is the specific surface area (SSA) of the electrodes in contact with electrolyte, ε_0 and ε_r values are the dielectric constants of the vacuum and electrolyte respectively, and d is the thickness of EDL [9][10].

It must be considered that the capacitance value from the equation 1 represents the value for one electrode/electrolyte interface, and because a symmetric supercapacitor contains two electrode/electrolyte interfaces connected in series, the total capacitance of the system is according to the equation 2 [3]:

$$\frac{1}{C} = \frac{1}{C_1} + \frac{1}{C_2}, \qquad \textit{Equation 2}$$

in which C_1 and C_2 are the capacitance values obtained from each electrode/electrolyte interface. The total capacitance of system affects the maximum stored energy in system based on the equation 3 [9]:

$$E = \frac{1}{2} C U^2, \qquad \textit{Equation 3}$$

where U is the maximum system voltage (V), and E is the maximum stored energy (J) of the supercapacitor. Similar to other electrical systems, there is a resistance in supercapacitors which is called equivalent series resistance (ESR). In general, different components of the supercapacitor affect the overall series resistance of the system such as the resistance of electrode material, current collector, and electrolyte. There are also other factors that contribute to the overall resistance such as the contact resistance between current collector and electrode, and ionic resistance of the electrolyte inside separator layer and porous electrode [9][3]. Figure 3 illustrates the voltage drop inside the electrolyte during discharge process [12].

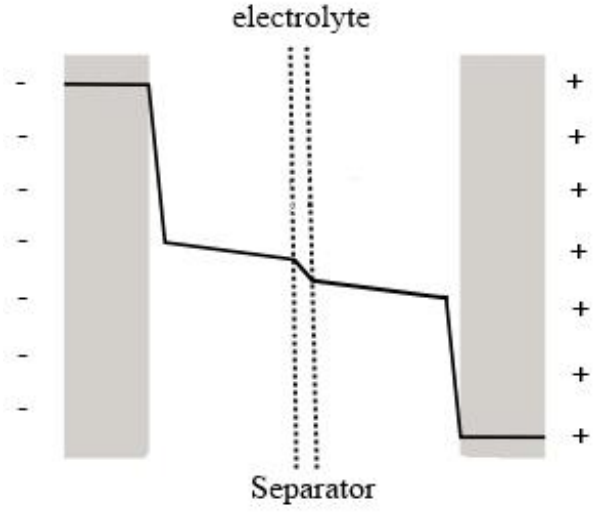

Figure 3. *Changes in voltage during discharge* [12].

The voltage drop inside the electrolyte arises from the ionic resistance of the electrolyte, and can be calculated by the equation 4 [12]:

$$V = IR, \qquad \textit{Equation 4}$$

where I is the discharge current, R is the resistance of electrolyte, and V is the voltage drop during discharge process. The equivalent series resistance (ESR) value of a supercapacitor alters the performance of the system by affecting the power based on equation 5 [1]:

$$P = \frac{R_L U_0^2}{(R_S + R_L)^2}, \qquad \textit{Equation 5}$$

in which P represents the maximum power (W), R_s is the ESR (Ω), R_L is the load resistance, and U_0 is the initial voltage of the system. The maximum power density of a supercapacitor occurs when the ESR and load resistance of the system are the same. Therefore, the equation 5 will be replaced by equation 6 [9][12]:

$$P_{max} = \frac{{U_0}^2}{4R_s}. \qquad \textit{Equation 6}$$

The stored energy in supercapacitors decreases with time in the open circuit state due to self-discharge in the component. The self-discharge is an important factor in the study of the duration for which the component is able to maintain the stored energy when it is not connected to an electrical circuit [13]. In general, three mechanisms contribute to the self-discharge of a component: Overvoltage of cell, Faradic impurity reactions, and Ohmic leakage current. In the first mechanism, the overvoltage of a cell beyond the voltage window of an electrolyte, results in the decomposition of the electrolyte and formation of gases. In the second mechanism, the presence of impurities results in a redox reaction, which alters the ion concentration on the electrode surface [1][13]. The last mechanism is the leakage current between two electrodes of the component, and is a result of electron conducting impurities [14]. To keep the component at constant voltage, charging current is needed to prevent voltage decrease. This current is called leakage current and it can be defined after different lengths of constant voltage periods, e.g. 1 hour or 24 hours [15][16].

2.1 The energy storage mechanisms of supercapacitors

The energy storage mechanism is dependent on the type of materials that have been used for electrode plates of a supercapacitor. Basically, there are two types of mechanisms: (i) electrical double layer (EDL), which is the capacitance obtained from electrostatic charge accumulation at the electrode/electrolyte interface, and (ii) pseudocapacitance which is the capacitance obtained from reversible redox processes at characteristic potentials. The total capacitance value is the sum of capacitance values from two mech-

anisms, although typically one of the mechanisms dominates the total capacitance [7][17].

2.1.1 Electrical double layer

The principle of double-layer capacitance is the storage of charge and formation of Helmholtz double layers at the electrode/electrolyte interface. The separation of charges at EDL results to a strong interactions between the ions/molecules in the solution and the surface of electrode. Figure 4 illustrates the EDL structure, in which inner layer closest to the electrode (also called Helmholtz, and compact layer) consists of the solvent molecules. This layer itself is divided to inner Helmholtz plane (IHP) and outer Helmholtz plane (OHP) [8]. The IHP contains the specifically adsorbed ions, which electrical center located at the distance of x_1. The OHP located at a distance x_2, and it represents the starting point of diffuse layer [9].

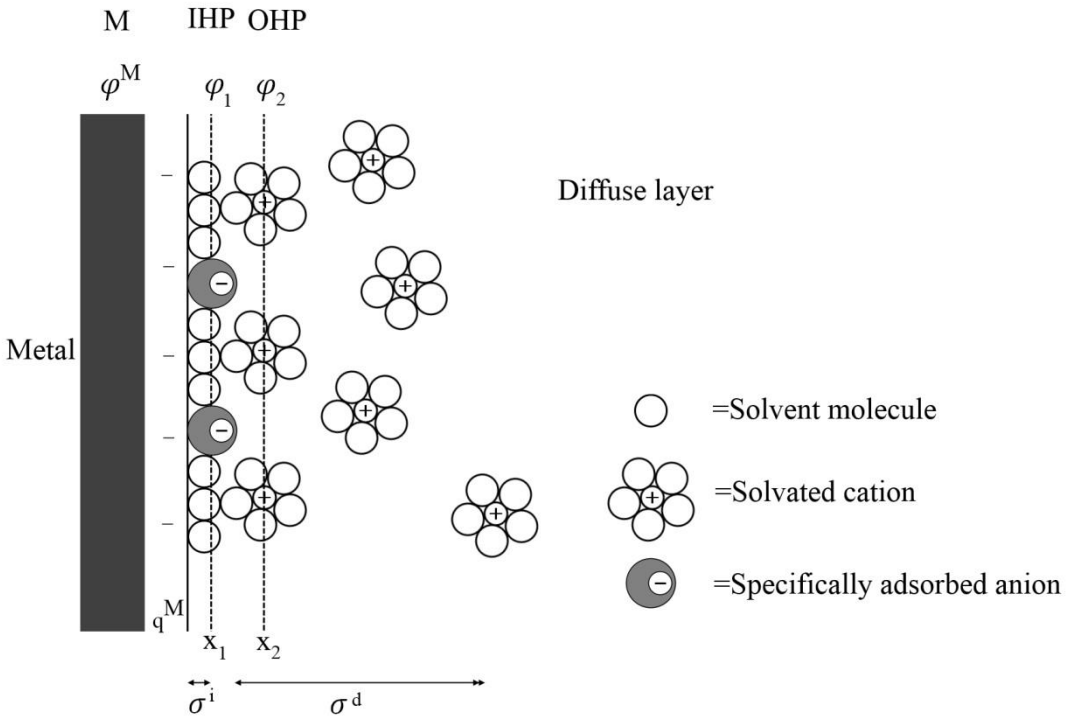

Figure 4. *Illustration of electrical double layer at the electrode/electrolyte interface* [6].

There are many factors that affect the behavior of EDL such as type of electrolyte, the accessible surface area for ions of electrolyte, and distribution of electrical field across the electrode [9]. In general, this type of energy storage mechanism is the dominant mechanism for carbon-based electrode material such as activated carbon (AC), carbon nanotubes (CNT), and graphene [10].

2.1.2 Pseudocapacitance

Pseudocapacitance is Faradaic in origin, and is based on fast and reversible redox reactions at the interface of electrode and electrolyte. The energy storage mechanism is similar to that of batteries, which is the transfer of charge. Pseudocapacitance results from the electrosorption of hydrogen or metal atoms, and strongly relies on the chemical affinity of the ions in the electrolyte to the surface of electrode [11]. Pseudocapacitance is the main energy storage mechanism for transition metal oxides such as MnO, RuO, NiO [17], and conducting polymers such as polyaniline, and polypyrrole [18].

2.2 Structure of supercapacitors

The common structure of a supercapacitor is a symmetric system of two electrodes immersed in an electrolyte, which are electrically isolated from each other by an insulating layer [3]. In order to obtain high performance in supercapacitors, each component of the system must have specific properties.

2.2.1 Electrode and current collector

In general, the electrode must be made of an electrically conductive material, which has a high surface area as well as high chemical and mechanical stability [19]. Moreover, the capacitance values of electrochemical double layer depend on the geometry of electrodes. In theory, a higher surface area of the electrode leads to higher capacitance values [20], due to the existence of more accessible area for charge carriers. However, in many practical cases higher surface area does not lead to higher capacitance values, because capacitance also depends on the pore size distribution. For example, the pores must be larger than ions in order to allow the ions to penetrate inside the pores [21]. Different classes of active electrode materials have been used in supercapacitors, such as activated carbon, carbon nanotubes, metal oxides, and conductive polymers [19].

Another important part in the structure of supercapacitors is the current collector. The function of this layer is to establish an electrical connection between an external source and the electrode of the supercapacitor. Therefore, the current collector must be made of conductive materials in order to minimize the ESR of the system. Moreover, there must be a low resistance contact between current collector and electrode layer [17]. In general, conductive metallic materials can be used as the current collector, and the most commonly used metal for this purpose is aluminum. A potential disadvantage of the metallic current collector is that the penetration of electrolyte toward current collector can lead to corrosion of this layer which affects the life-time of the component. Corrosion of current collectors occurs in supercapacitors with aqueous electrolyte, but not in components with organic electrolytes.

2.2.2 Electrolyte

In a supercapacitor system, the electrolyte acts as an ionic conductive medium between electrodes. The electrolyte material must be carefully chosen in order to maximize the operating voltage, which leads to higher power and density values of the system [10]. In general, a suitable electrolyte must be ionically conductive, with wide voltage window, and high chemical and thermal stability. Moreover, electrolyte solutions with lower viscosity are preferred because of the higher mobility of ions in the electrolyte. There are different types of electrolyte such as organic, aqueous, and ionic liquids. The main advantage of organic electrolytes is their wide voltage range, e.g., 2.7- 2.8 V which makes them suitable for industrial applications [3]. However, these electrolytes are not environmentally friendly, and they deliver low power densities due to their high resistivity values [22]. While aqueous electrolytes only sustain voltage of 1.2 V, they are environmentally friendly, low cost, and show low resistance values [23]. Another advantage of aqueous electrolytes over other electrolytes is their small ion size. Smaller ion size leads to higher effective surface area, as ions can access smaller pores in the electrode material [24].

2.2.3 Separator

The separator is a porous dielectric which is placed between anode and cathode to prevent short circuit in the system. At the same time, it enables diffusion of ions and electrolyte molecules. The separator must be chemically and mechanically stable, with high wettability, and high permeability. High permeability values of the separator lead to ease of ion movement through this layer [17][25]. Moreover, this layer must be able to withstand the voltage window of the used electrolyte, without losing the main characteristics.

3. ELECTRODE MATERIALS

Successful designs of electrode materials for supercapacitor applications lie into having following properties:

1. **High specific surface areas**:
   In general, in a porous structure smaller porosities give a rise to specific surface area of the material. Theoretically, the area for formation of electrical double layer (EDL) is higher in materials with higher specific surface area [12]. Although, there is not a linear relationship between specific surface area and capacitance values of carbon materials [26].
2. **Proper accessibility of electrolyte to intra-pore surface area**:
   Ideally, the size of pores must be big enough, in order to bring sufficient volume for accommodation of electrolyte [12]. In other words, engineering a matrix structure with an optimum pore size that fits with the ion size of electrolyte is a key factor for obtaining high capacitance values [3].
3. **Proper size distribution of pores in the matrix structure**:
   Proper size distribution of pores ensures that there is a proper intra-and inter-particle conductivity in porous materials [12].

Although use of porous materials brings many advantages for supercapacitor applications, it has a number of drawbacks such as non-uniform charge distribution, and high contact resistance inside the porous structure. In general, when the porous structure filled with electrolyte is subjected to an external electrical stimulus, such as current or potential, the available electrode area in the matrix is not charged simultaneously at a uniform rate inside the matrix. The non-uniform distribution is a result of ohmic resistance associated with electrolyte filling pores [12].

Preparation methods of carbon materials play an important role in the functionality of the electrode of a supercapacitor. Different preparation methods result in different surface condition and properties of carbon materials. Preparation methods are involved with different steps such as high temperature pre-treatment, exposure to different atmospheric situations, and surface modification of material [12]. The effect of each preparation step on the properties of the electrode material of supercapacitors is as follow:

1. **High temperature pre-treatment**
   Heat treatment of carbon powder results in a higher degree of crystallization, which lead to decreased inter-particle contact resistance. Moreover, heat-treatments are expected to open the pore structure, which is beneficial for for-

mation of double layer. Another function of heat treatment of the carbon powder is to remove oxygen functional groups, which exist on the surface of carbon [22]. The function of oxygen functional groups will be explained in following pages.

2. **Exposure to different environments**
   Depending on the preparation method of carbon, the process may involve exposure of material to different atmospheric conditions. These conditions can be a part of the production process (e.g. oxidation-reduction of graphene oxide), or can be used for the modification of carbon (e.g. removal of oxygen functional groups) [12].
3. **Surface modification**
   In general, surface modification of electrode material affects the surface functionalities, concentration of impurities, pore structure, and wettability of the sample by electrolyte [12]. Although the purpose is the improvement of performance, it has been reported that the surface modification may lead to negative effects such as increased junction resistance between particles [27].

Different types of oxygen functional groups are present on the surface of carbon, and might be introduced to the surface of carbon electrode during the operation of supercapacitors, especially in the case of system over-voltage. Figure 5 represents some of these functional groups. The presence of oxygen functional groups is a result of the bond between oxygen and unpaired electrons, which exist in the imperfect crystals of carbon.

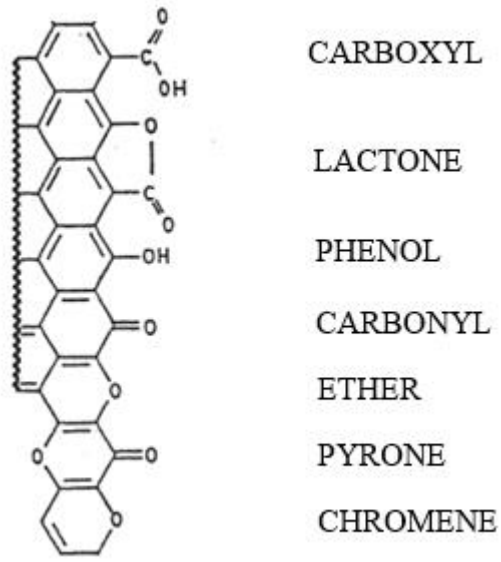

Figure 5. *Oxygen functional groups on the plane of carbon* [22].

The oxygen functional groups affect the performance of the electrode material of supercapacitors by causing electrochemical reactivity, changing wettability properties of the electrode, and changing the self-discharge characteristics of a supercapacitor. In gen-

eral, the wettability of electrode by electrolyte is higher when there is increased oxygen content. In other words, these functional groups decrease the contact angle between the electrolyte and electrode, especially in the case of aqueous electrolyte [22]. Another effect of oxygen bonds is increased inhomogeneity in the crystallographic orientation of carbon, which leads to increased time-dependency of charge distribution on carbon surface. In other words, in an electrode with oxygen functional groups the spread of charge to different points of the surface does not occur simultaneously. Moreover, the presence of these functional groups in the electrode material leads to increased self-discharge of the EDLC [28]. In other words, the oxygen functional groups cause Faradaic reactions. These Faradaic reactions consume charges, which are accumulated across the electrode material. Therefore, these functional groups must be avoided in EDLC [20].

In supercapacitors made from porous materials, it is common to report capacitance values as a function of electrode mass. This value is known as specific capacitance and has the unit of F/g [9]. As explained in chapter 2, with the assumption of the component being symmetrical the total capacitance of a supercapacitor is 50% of the capacitance of each electrode. When defined as specific capacitance values, the specific capacitance value of a whole component is 25 % of the specific capacitance of single electrode since the capacitance is decreased by 50 % due to series connection of the two double layers and simultaneously the mass of active material is doubled.

3.1 Graphene

Graphene is a two dimensional (2D) monolayer of carbon atoms, and is the basic building block of graphitic materials such as carbon nanotubes (CNT) and graphite [29]. In a two dimensional crystalline structures of graphene, carbon atoms are packed into a hexagonal crystalline structure and each carbon is connected to its three nearby neighbors by strong σ bonds. The nearest neighbor interatomic distance in this structure is 1.42 Å [29][30]. Figure 6 illustrates the structure of graphene.

The planar σ bonds between carbon atoms occur based on the occupation of sp^2 orbitals by three valence electrons [31], while the π bonds are the perpendicularly oriented bonds to the plane of graphene. These π bonds are responsible for the electronic characteristics of graphene [30].

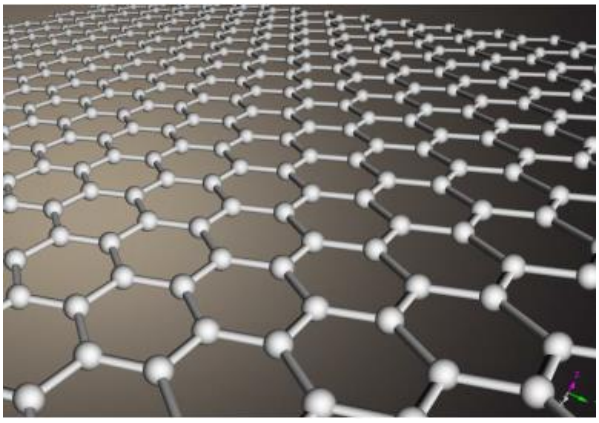

Figure 6. *The hexagonal crystalline structure of graphene* [24].

Theoretically, a monolayer plane of graphene has a high electrical mobility of 200,000 $cm^2/(V•s)$ [24]. Altering the number of layers affects the electronic properties. In general, single layer graphene (SLG) and double layer graphene (DLG) act as zero-gap semiconductors, while in few layer graphene (FLG 3 to <10) the overlap of valence and conduction bands change the electronic properties [30]. When the number of layers is more than 10, the electronic structure evolves to the three dimensional (3D) limit of graphite.

A single layer of graphene has a specific surface area of 2675 m^2/g, and can have specific capacitance up to ~550 F/g [24]. The effective surface area of graphene depends strongly on the number of layers [32]. In single layer graphene, both sides of the plane are available for charge storage, and surface area has the highest theoretical value [33][1]. Increasing the number of planes causes a decrease in effective surface area of graphene [32]. For supercapacitor applications, graphene has an important advantage in comparison to other carbon based materials: the effective surface area of graphene materials does not depend on the distribution of pores at solid state [32]. Therefore, preparation of graphene based supercapacitors should be in principle less complicated than activated carbon and CNT based supercapacitors [21].

The electrochemical characteristics of graphene can be altered by edge structure. Figure 7 illustrates two possible types of edge structure in the graphene plane, namely armchair and zigzag. In general, the reactivity of zigzag edge structure is higher than that of armchair structure. Moreover, defects are considered as reactive sites in the graphene lattice. The reactive sites in the graphene structure have a higher tendency to adsorb solvent molecules, which result in the distortion of the graphene lattice and consequently change of charge transport characteristics [34]. The quality of crystal also affects the electrical conductivity of graphene. For example, lattice imperfections and defects in the crystal affect the charge transport characteristics, and act as scattering sites in the free path of electrons [29].

Moreover, the electrochemical behavior of the basal plane is different from that of edges. W. Yuan et.al [35] have reported that graphene edges exhibit larger specific capacitance, and faster electron transfer rate than those of the basal plane. In case of multilayer graphene, the presence of surface functional groups and defects in graphene sheet not only leads to pseudocapacitance, but also results in the wrinkling of the sheet [36][37]. Folding of graphene sheet reduces the area of contact between parallel sheets, and also prevents sheets from being stacked on the top of each other [37]. C. Liu [33] has shown that the shape of graphene sheet affects the performance of graphene-based supercapacitor. By comparison of the shape of graphene sheet, it has been stated that by changing the shape of graphene to curved planes, the capacitance increases. In other words, curved sheets exhibit less agglomeration and stacking of sheets, and consequently higher effective surface area of the electrode material.

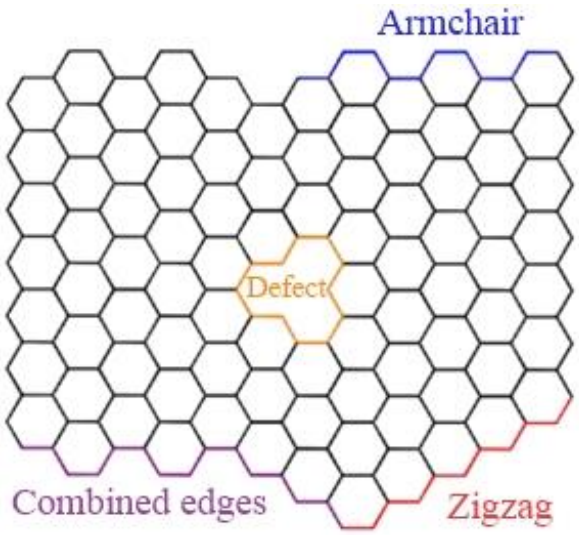

Figure 7. *Illustration of graphene crystal in the presence of defect and different edge structure* [34].

The preparation method of graphene affects the final properties of the electrode material. Many different approaches have been used for preparing graphene including epitaxial growth, graphitization, exfoliation, and chemical vapor deposition (CVD) [38]. One of the most effective methods in mass production of graphene is the oxidation and reduction of graphite, although graphene made by this method exhibits an irreversible agglomeration and precipitation of graphene particles, and also degradation of electrical conductivity [24][39].

3.2 Activated Carbon

Activated carbon is a porous structure of carbon, comprising small hexagonal rings of graphene sheets. In these materials, there is a limited order between graphene sheets. The stacking, orientation, and the size of graphene sheet are directly related to the preparation method of activated carbon [40]. In activated carbon the distribution of pore size

is large and consists of macropores (>50 nm), mesopores (2–50 nm), and micropores (<2 nm). The dominant surface area of AC is on the scale of micropores [2]. Figure 8 presents the structure of these pores.

As stated earlier, pore size and pore size distribution affect the performance of supercapacitors. In case of activated carbon, presence of macropores does not contribute to the adsorption of electrolyte molecules, and the main effective surface area for EDLC arises from the presence of mesopores. However, their presence is necessary during activation process as they act as a path for oxidizing agents, which lead to formation of mesopores and micropores [1]. In EDLC, the most of contribution to the formation of double layer is from mesopores. Micropores are incapable of supporting double layer, as they are non-accessible for electrolyte ions (especially in case of organic electrolytes) [2].

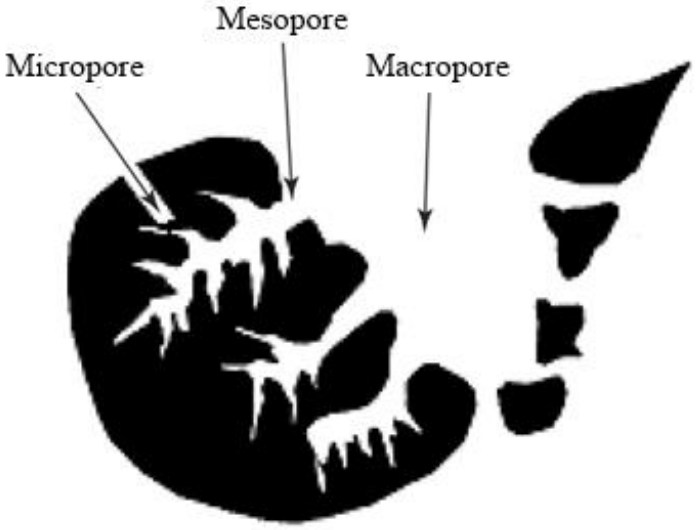

Figure 8. *An schematic of macropore, mesopore, and micropores of AC* [1].

Depending on the structure of activated carbon, the specific surface area ranges from 500 to 2000 m^2/g. Although the specific surface area values of activated carbon are high, the inaccessibility of micropores for electrolyte results in small specific capacitance of 160 F/g in aqueous electrolyte and 100 F/g in organic electrolytes [24].

One of the main problems with activated carbon is the difficulty in controlling the pore size and pore size distribution, which limits the performance of AC in EDLC supercapacitors [41]. Moreover, the porous structure of AC hinders the high electrical conductivity in these materials [2].

Activated carbon can be obtained from natural sources such as coconut shells, coke, wood, or from synthetic polymers. The activation of carbon is an important step in the production of activated carbon, as it has a direct effect on the porous structure of AC. The activation process involves heat treatment of a carbon-rich precursor in the presence of an inert atmosphere. The process continues with a physical or chemical activa-

tion for development of surface area [1]. The physical activation uses a gaseous agent, whereas in the chemical approach the activating agent is a solid [42]. The physical activation is based on controlled gasification of carbon precursor with CO_2 or steam according to equations 7 and 8 [1]:

$$C + CO_2 \rightarrow 2CO, \qquad \textbf{Equation 7}$$

$$C + H_2O \rightarrow CO + H_2. \qquad \textbf{Equation 8}$$

Another approach for activation of AC is chemical activation. The chemical activation is based on formation of redox reaction of chemical species with carbon, followed by intercalation and expansion of the structure. Several chemicals can be used in this approach such as KOH, $ZnCl_2$, and H_3PO_4 [1]. An advantage of chemical activation over physical activation is the low process temperature. However, in activated carbon prepared by chemical activation there is a higher content of oxygen functional groups, which results in pseudocapacitance in the component [42]. During the activation process, changes in treatment temperature and activation time affect properties such as surface area, pore size, and yield of carbon [43].

In flexible electronics applications, preparation of electrode material is based on the mixture of AC powders with an organic binder. In general, the binder has two main functions, namely cohesion of AC particles and promotion of adhesion of electrode to current collector. The mixture of AC and binder is in the form of paste or ink to be printed onto the current collector. The choice of a suitable binder is important, as it alters properties of the electrode material. For example, binders are insulating polymers and electrodes with high content of binder suffer from an increase in the ESR of supercapacitor. Moreover, intergranular space in the electrode might be blocked by the binder. Therefore, the content of binder must be controlled precisely [1].

Electrochemical characteristics of AC are affected by the purity of electrode material. For example, presence of heavy metals results in self-discharge and short circuit of the component. Therefore, the native AC powder must be purified. Moreover, the presence of elements such as iron, potassium and chloride leads to unstable behavior of the electrode material over a long period of time [1]. In a similar way to graphene materials, the presence of functional groups in activated carbon has an impact on the performance of supercapacitors. These functional groups cause an increase in the resistance of electrode. Moreover, they increase the total capacitance of the component by introduction of pseudocapacitance, resulting from redox reaction of surface groups [1]. Nakamura et. al [44] showed that in a AC electrode with high content of oxygen, production of gas leads to deterioration of component reliability during charging. They also claimed that the presence of acid groups in activated carbon is harmful, especially in the case of aqueous media. In general, acid groups result to an increase in leakage current, and significantly reduce the lifetime of the supercapacitor.

V. Ruiz et. al [45] reported that heat treatment of AC is beneficial in EDLC applications. In other words, the heat treated samples has shown better long term stability, less capacitance loss after 10000 cycles, but less capacitance values compared to un-treated samples. It has been explained that heat treatment removes oxygen functional groups, which is responsible for higher stability and lower capacitance. Moreover, heat-treated samples do not show pseudocapacitance. In another study [42], it has been shown that the removal of oxygen functional groups with microwave treatment is more efficient compared to heat treatment in electric furnace.

3.3 Carbon Nanotube

Carbon nanotube (CNT) is a cylindrical structure, which is made of the wrapped up hexagonal lattice of graphene sheet. Based on the number of cylinders, CNTs can be categorized into different structures namely single wall nanotube (SWNT), double wall nanotube (DWNT), and multiwall nanotube (MWNT). In SWNT the diameter of tubes is in the order of 1-2 nm, while in a MWNT, cylinders are concentric with interlayer spacing of 0.34 nm and diameters in the order of tens of nanometers. Figure 9 illustrates the structure of SWNT and MWNT [46].

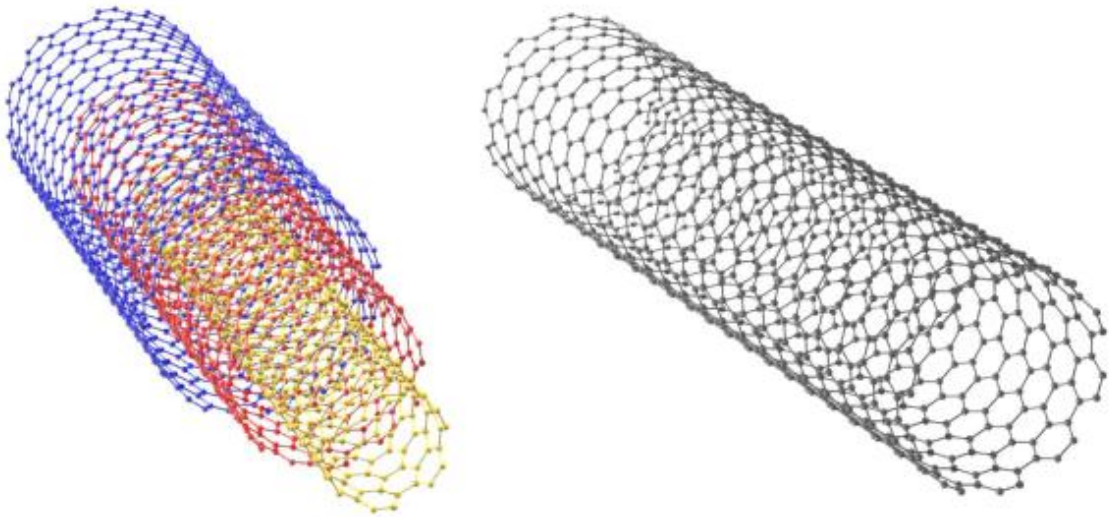

Figure 9. *Illustration of MWNT (left) and SWNT (right)* [47].

Depending on the structure of nanotubes, they can act as metallic or semiconducting materials. In general, MWNTs are all metallic and SWNTs are either metallic or semiconducting. Moreover, the electrical properties of CNTs depend on structure parameters such as chirality [46]. Chirality can be defined as the “twist” in the structure of CNT, and is based on the angle at which a graphene sheet is rolled up. As shown in figure 10, different twisting angles result to different structures of CNT such as chiral, zigzag, and armchair. Generally, chirality can be presented by a vector (n,m). This vector contains information about twisting angle of CNT structure, as well as diameter of

tubes. Moreover, this vector can be used to determine electrical properties of CNTs. It has been stated that the electrical properties of CNT are similar to metallic materials when |n-m|=3q, in which q is an integer value [48].

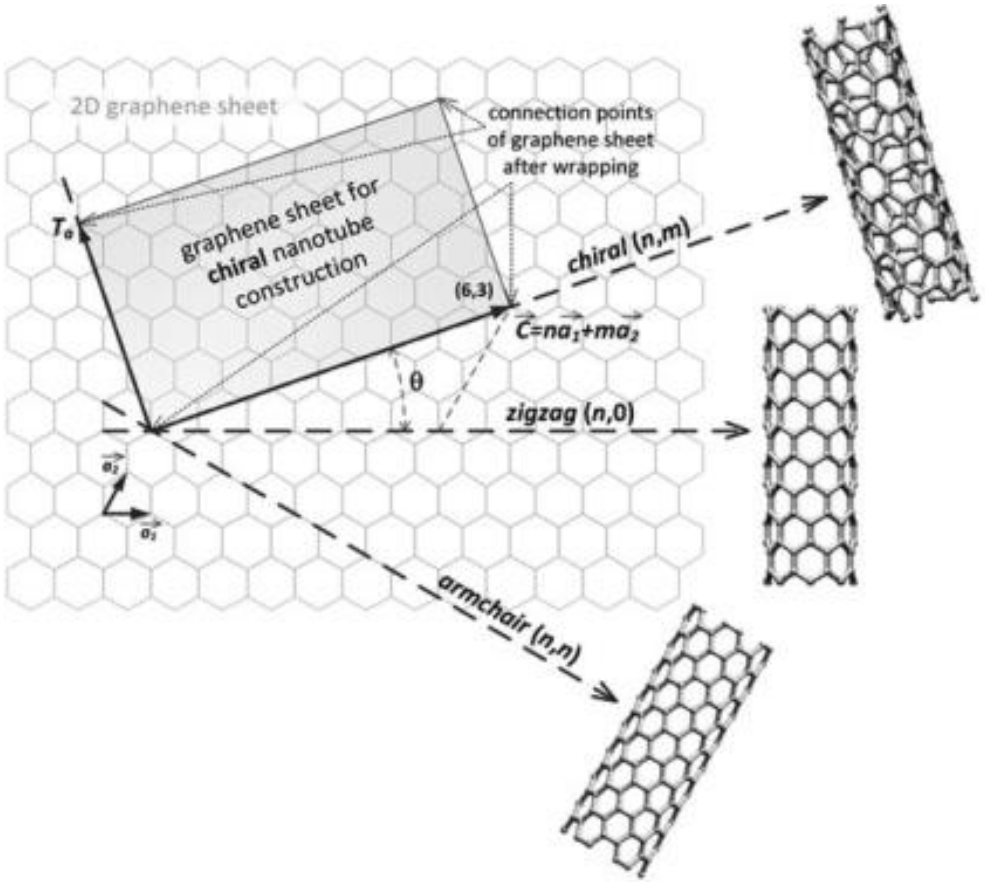

Figure 10. *Different structures of CNT based on the rolling angles of graphene sheet* [49].

The electrical conductivity of metallic SWNT is in the order of 10^4 S/cm [46], and the specific surface area of an individual SWNT is 1315 m^2g^{-1} [50]. The size distribution of pores in CNT is in the range of mesoporous rather than micropores [21][51]. The double layer capacitance of SWNT-based supercapacitors has a wide range between 20 to 300 F/g [52]. In case of MWNT-based supercapacitors, capacitance values up to 135 F/g were reported in aqueous based supercapacitors [21].

Similar to other carbon based electrode materials, specific surface area affects the capacitance of CNT based supercapacitors. In other words, capacitance depends on the diameter of tubes, arrangement of nanotubes, and accessibility of ions to the internal surface of tubes [21]. Moreover, number of layers in CNT affect the surface area and consequently capacitance of the component [46]. A. Peigney et al [50] calculated the theoretical values of specific surface area of bundled CNTs. As can be seen in figure 11, the specific surface area is directly related to the number of nanotubes and decreases with increasing number of nanotubes.

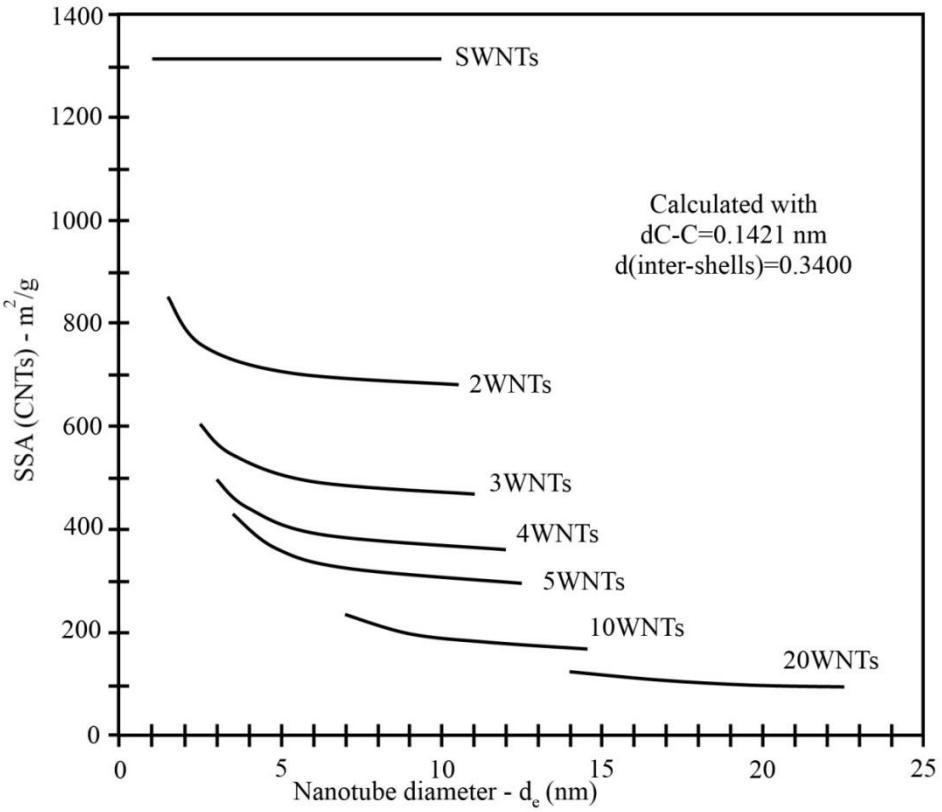

Figure 11. *Changes in specific surface area as a function of nanotube wall numbers* [50].

Although the surface area of CNT electrodes is lower than AC electrodes, easy accessibility of electrolyte ions to mesopores of CNT lead to lower ESR values of CNT electrodes compared to AC electrodes [24]. However, the values of resistance at the electrode/current collector interface of CNT-based supercapacitors is usually high [32].

In general, values of capacitance for SWNTs are higher than for MWNTs, which can be explained by the high surface area for SWNTs. However, Frackowiak et al [53] showed that MWNTs could generate higher capacitance values than that of SWNTs after certain modifications. The higher capacitance of MWNTs resulted from increased accessibility of central canals, as well as introduction of pseudocapacitance.

In carbon nanotubes the aspect ratio is usually more than 1000, which leads to entangled structure of nanotubes to form a porous skeleton. As the result, open spaces between nanotubes can be easily accessed by electrolyte ions [46]. However, depending on the size of ions in electrolyte, a randomly entangled structure of CNT might be detrimental [2]. Wen Lu et al [54], have investigated the effect of CNT alignment on the performance of supercapacitors with ionic liquid electrolyte. It has been shown that aligned structure of CNT leads to increased capacitance values.

In printable electronics, processing of CNT usually involves several challenges. For example, the concentration of CNT in water or organic solvents is usually limited to low values [55]. Moreover, CNTs tend to aggregate due the van der Waals interaction, which result to reduction of surface area of the electrode material [55][56]. Therefore, it is challenging to produce dispersions with high concentrations of CNT even after modifications of CNT [55].

In order to improve dispersion properties of CNTs, different approaches can be used. One approach is the addition of surfactants with hydrophilic head and a hydrophobic tail. Surfactants can be adsorbed to each CNT from their hydrophobic tail. In this way, the adsorbed hydrophobic tail acts as a physical barrier between CNTs to negate van der Waals forces. Another approach is the addition of long chain polymers that wrap around nanotubes, to act as both chemical and physical means to overcome van der Waals forces [57]. However, it must be considered that formation of physical barriers around CNTs leads to decreased conductivity, as those barriers inhibit the contact between CNTs.

Generally, a dried printed layer of carbon nanotubes consists of a random network of nanotubes. Therefore, very often it is possible that some of the nanotubes are isolated form other nanotubes in the network. Those isolated nanotubes do not contribute to the conductivity of the printed film. On the other hand, connected nanotubes lead to creation of electron pathway and consequently increase conductivity of the printed film, as shown in figure 12. Therefore, it is expected that in a printed thin film with long CNTs conductivity is higher than in a film constituted from short CNTs [57].

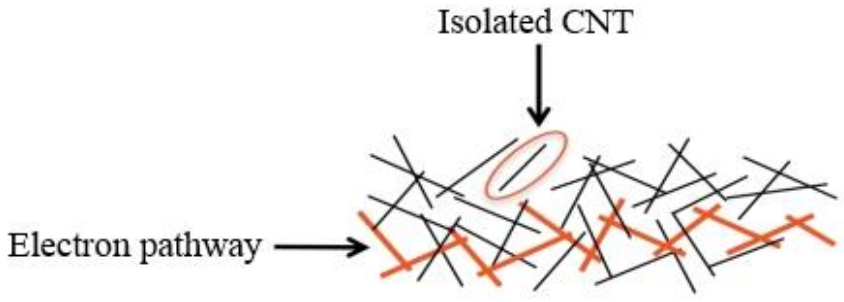

Figure 12. *Formation of electron pathway from the connection of CNTs* [57].

4. CHARACTERIZATION OF ELECTRICAL PROPERTIES

The electrical performance of supercapacitors can be determined from measurement methods such as cyclic voltammetry, and galvanostatic measurements [58]. The main objective of these measurements is to determine properties such as capacitance, leakage current, equivalent series resistance (ESR), and cycle life of the supercapacitors. There are different standards for the measurement of supercapacitors. In this study, all the electrical measurements except cyclic voltammetry are based on the IEC 62391-1 standard [15]. The detailed information about specification of standard in each method will be presented in the following part.

4.1 Cyclic Voltammetry

Cyclic voltammetry is a common method in measurements of electrochemical cells, and it is based on the cycling of potential in a cell, and measurement of the resulting current [59]. Cyclic voltammetry yields information about capacitance, cycle life, and general performance of a tested supercapacitor [12]. A typical CV curve of an ideal supercapacitor can be seen in figure 13.

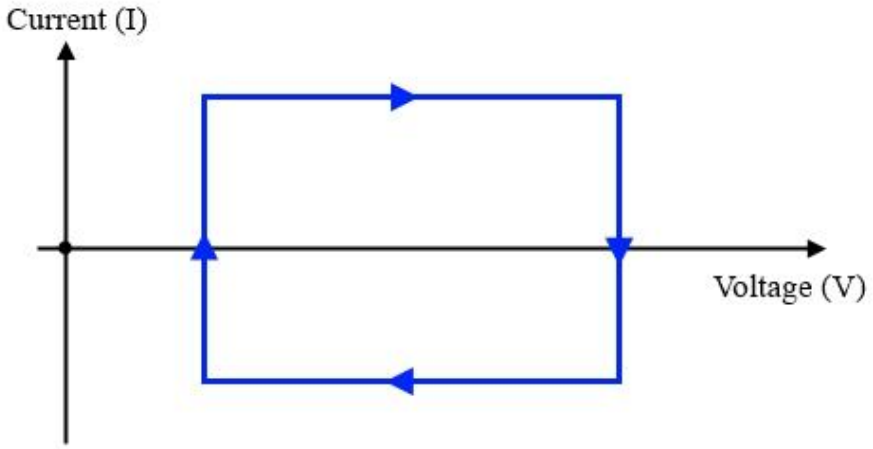

Figure 13. *Cyclic voltammetry diagram of an ideal supercapacitor*

The rectangular shape is characteristic of charge storage for a pure double layer capacitance mechanism, and it is based on equation 9 [60]:

$$I = C \times \frac{d_v}{d_t}, \qquad \textit{Equation 9}$$

where C is the double layer capacitance, I is current, and d_v/d_t is the potential scan rate [60]. Practical supercapacitors do not exhibit the rectangular behavior in CV curves, as there is an ESR and leakage current in all practical supercapacitors. The changes in the diagram for each case can be seen in figure 14 [23].

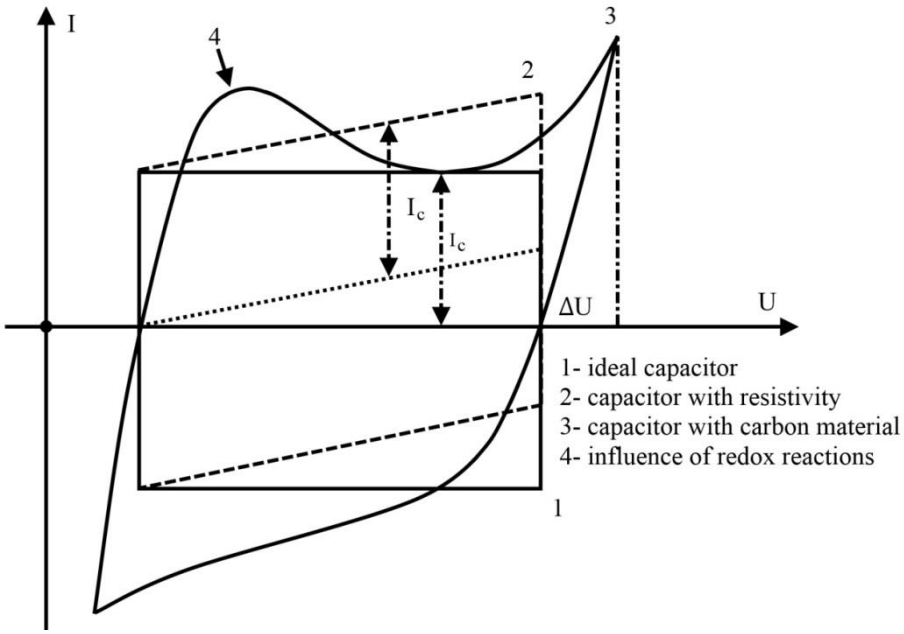

Figure 14. *Comparison of CV diagram of ideal supercapacitor and practical supercapacitors*

In this figure, the sharp peak at the end of CV curve for carbon materials represents the leakage current of component. Moreover, in supercapacitors with pseudocapacitive properties redox reactions appear as a peak in the voltage windows of the measurement.

In CV measurements, the capacitance value of EDLC depends on the potential scan rate. It arises from the fact that in higher rates, charged particles cannot penetrate into the accessible pores which results to a decrease in capacitance values [61].

4.2 Galvanostatic charge-discharge

Another method for evaluation of capacitance is galvanostatic measurement. In this method the supercapacitor is charged and kept at a constant voltage, and measurement continues with discharge at a constant current. The schematic of this process has been illustrated in figure 15:

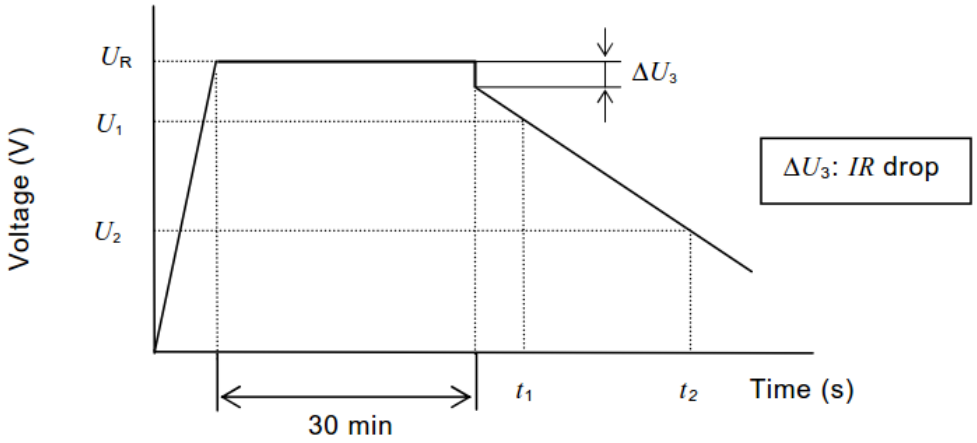

Figure 15. *Illustration of galvanostatic measurement process* [15]

In this measurement capacitance can be calculated based on equation 10:

$$C = \frac{I \times (t_2 - t_1)}{U_1 - U_2}, \qquad \textit{Equation 10}$$

in which C is capacitance, I is the constant current during discharge, U_R is the maximum voltage, U_1 is the 80% of the maximum voltage, and U_2 is the 40% of the maximum voltage during discharge process. Moreover, this method yields information about ESR and leakage current values. As it can be seen in figure 7, at the beginning of the discharge process there is a sudden drop in voltage, which presents the IR drop of the component. The ESR can be calculated from the equation 11:

$$ESR = \frac{\Delta U_3}{I}, \qquad \textit{Equation 11}$$

where I represents the current during discharge process, and ΔU_3 is the IR drop.

For the measurement of leakage current, similar charge-discharge measurement can be applied. The only difference is that the duration of charging with constant voltage is 20 hours for this measurement. The leakage current is the value of the current at the end of the constant voltage step [15].

4.3 Sheet resistance measurement

In printable electronics, the resistance of a conductive film is often specified as sheet resistance (R_S). The unit of sheet resistance is Ω/sq, and this value is always defined for a certain layer thickness. A common method for measurement of sheet resistance is the four-point measurement. In this method, a probe with four connections must be placed on the electrode surface. Two outermost connections apply a current to the electrode, and two innermost connections measure the resulting voltage [62]. Figure 16 shows a schematic diagram of a probe for the four-point measurement.

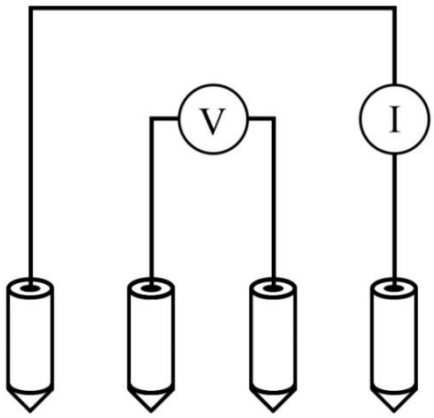

Figure 16. *Illustration of probe configuration for Four-point measurement*

The sheet resistance values of the sample can be calculated based on equation 12 [62]:

$$R_S = \frac{\pi}{ln2} G \frac{V}{I}, \qquad \textbf{\textit{Equation 12}}$$

in which V is the voltage, I is the current, and $\frac{\pi}{ln2} G$ is related to the geometric correction factor of the measurement. The geometric correction factor of different shapes can be found in literature [63].

5. MATERIALS AND METHODS

This part of the thesis consists of the description of procedures for fabrication and electrical characterization of supercapacitors, assembled with different materials and with different component designs.

5.1 Materials

All the electrode materials were in the form of ink, and were printed on polyethylene terephthalate (PET) substrate. The assumption in this work was to prepare supercapacitors with suitable flexibility. In some experiments, PET substrates with a layer of copper on the surface have been used. The copper-coated substrates were chosen in order to test the functionality of copper as the current collector of supercapacitors. The detailed information about substrates can be seen in table 1.

Table 1. *Specification of utilized substrates*

Substrate	Company	Code	Thickness of substrate	Coating Method	Thickness of Coating
PET	Dupont Teijin Films	Melinex 506	125 µm	N/A	N/A
PET coated with Copper	Dupont Teijin Films	Melinex 506	125 µm	Sputter Coating	100 nm

In addition to copper current collectors, two other materials were tested for this function, namely graphite and silver. These current collectors were deposited as inks onto, PET substrates by doctor blading and inkjet coating, respectively. Detailed information about the current collectors and coating methods can be seen in table 2.

In some components, combination of different current collectors was used. The detailed explanation about the combination of current collectors will be presented in chapter 5.2.1.

Table 2. *Specification of current collectors*

Current Collector	Company	Code	Viscosity (mPa.s)	Coating Method	Drying Temperature and Time	Sheet Resistance values (Ω/sq)
Graphite Ink	Henkel	Electrodag PF-407 C	42500	Doctor Blade	90°C 30 Minutes	11
Silver nanoparticle Ink	Harima	NPS-J	7-11	Inkjet	130°C 1 Hour	0.2

Two different separators were utilized for the assembling of supercapacitors. Information about separators is presented in table 3. The criteria for the selection of separator were wettability by electrolyte, suitable porosity, and good mechanical strength. Considering the mechanical properties of the wet separator, Dreamweaver shows better properties in comparison to NKK separators. Therefore, Dreamweaver separator was chosen as the main separator of supercapacitors.

Table 3. *Specification of separators*

Company	Product's Code	Thickness
NKK	TF4050	50 µm
Dreamweaver	Silver AR40	40 µm

Preparation of electrode was done by utilizing three categories of inks made of activated carbon, graphene, and CNT. Except activated carbon, the rest of electrode materials were provided in the form of ink. In the case of CNT inks, ten different inks were tested as the electrode material. The detailed Information about CNT and graphene inks can be seen in table 4.

Table 4. *Specification of electrode materials*

Ink Code	Provider Company	Material	Percentage of active material	Drying temperature and time	Sheet Resistance value (Ω/sq)
NT20/V2010	Morphona	CNT	2%	100°C 10 Minutes	37
NT20/S8010	Morphona	CNT	2%	100°C 10 Minutes	30

Ink Code	Provider Company	Material	Percentage of active material	Drying temperature and time	Sheet Resistance value (Ω/sq)
NT40/S8020	Morphona	CNT	4%	100°C 10 Minutes	14
BT50L20	Morphona	CNT	5%	100°C 10 Minutes	59
BT50/S8010	Morphona	CNT	5%	100°C 10 Minutes	50
Bristol	Bristol	CNT	N/A	Room temperature 24 Hours	10.5
NL30XU15	Morphona	CNT	N/A	100°C 10 Minutes	78
NC30H8020	Morphona	CNT	N/A	100°C 10 Minutes	89
NC30S8015	Morphona	CNT	N/A	100°C 10 Minutes	34
X103	Vor-ink™	Graphene	N/A	120°C 4 minutes	9

All the Morphona CNT inks were made of multi-wall nanotubes (MWNTs). No further information was provided by the producers, as the information about the constitution of inks was confidential.

For the preparation of activated carbon ink, a mixture of acetic acid, chitosan, water, and activated carbon powder was used. The detailed quantities of components can be seen in the table 5. Preparation of the ink started with dilution of acetic acid with 60 g distilled water. Next, chitosan was added to the solution, and followed by agitation with a magnetic stirrer for 20 hours. The last step was the addition of activated carbon powder to the solution, and followed by stirring with ultrasonic rod for 10 minutes. The carbon powder was provided by Kuraray Ltd. In all the steps of ink preparation, it is important to make sure that there is a minimized agglomeration of particles.

For all the supercapacitors of this work, a 1M sodium chloride (NaCl) solution was used as the electrolyte material. The idea was to use an environmentally friendly electrolyte. The quantity of electrolyte for each component was between 0.3 to 0.4 gr.

Table 5. *Quantity of materials for preparation of activated carbon ink*

Material	Water	Chitosan	Activated Carbon	Acetic Acid
Quantity	90 g	1.7 g	30.9 g	0.7 g

Sealing of supercapacitors was done by using two different approaches. In the first approach, an adhesive tape and in the second approach a sealing liquid was used. The detailed information about sealing procedure will be explained in another section (see 5.2.5). Table 6 presents the specification of sealing materials.

Table 6. *Specification of sealing materials*

Sealing material	Provider Company	Drying time and temperature	Thickness
Adhesive Tape	NKK	N/A	N/A
Aquaseal X 2277	Paramelt	30 minutes at 80°C	*N/A*

For coating of CNT samples on PET substrate, there was a need for surface modification of PET substrate, in order to increase the adhesion of CNT to the substrate. The modification was done by using Edolan dispersion. Edolan is an aqueous polyurethane dispersion, which was provided by Tanatex chemicals.

5.2 Procedure

5.2.1 Component design

The first step in the preparation of supercapacitors was designing the component. Depending on the type of current collector materials, three different architectures were designed. In the first architecture, the current collector and the electrode were prepared with graphene ink. The structure of each plate of supercapacitor for this architecture can be seen in figure 17.

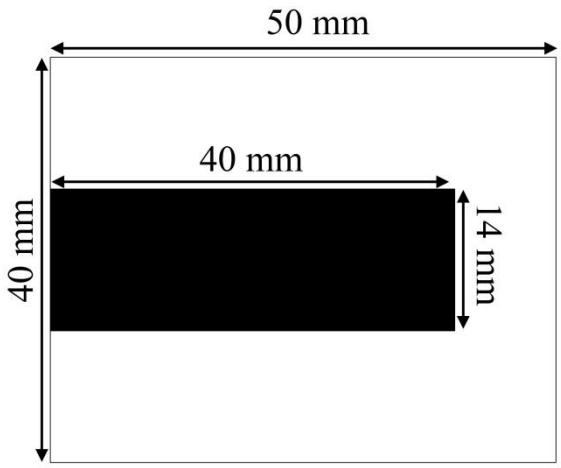

Figure 17. *The structure of a substrate coated with graphene (gray area).*

In this architecture two plates of the supercapacitor were perpendicular to each other and the common area between two electrodes was 14*14 mm^2. An example of the component design can be seen in the figure 18.

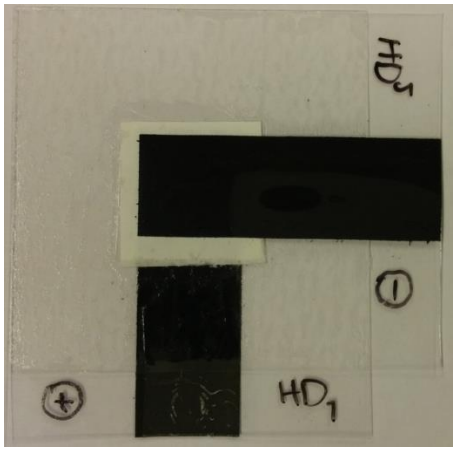

Figure 18. *The supercapacitor designed based on the first architecture.*

In the second architecture, silver was coated on the substrate and a layer of graphene was coated on top of silver layer. Both layers in this structure act as the current collec-

tor. The reason for combining two layers was to decrease the resistance of the current collector. The main function of the graphite layer was to protect silver from being corroded. Figure 19 illustrates the structure of a coated substrate.

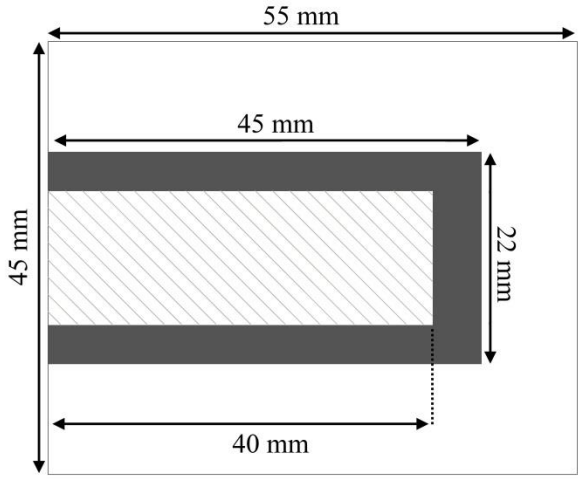

Figure 19. *The structure of a substrate coated with Silver (gray area) and Graphene on the top (black area).*

The electrode material used in this architecture was activated carbon. AC was applied onto the graphene layer, on the common area of silver and graphene current collectors with the dimensions of 14*14 mm^2. Figure 20, illustrates the structure after addition of AC.

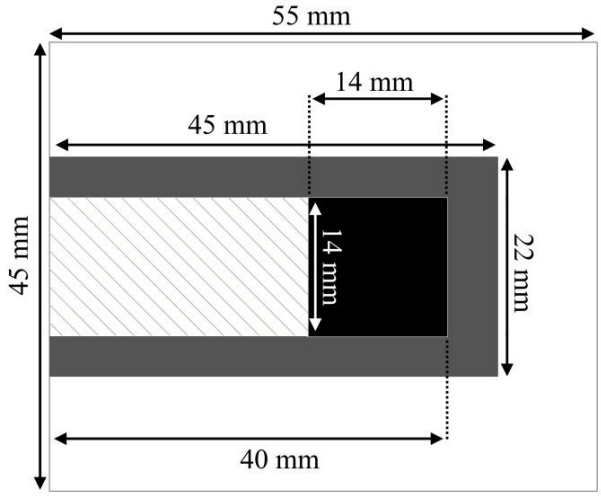

Figure 20. *The substrate after coating with AC (dark black area) with dimensions of 14*14 mm.*

Two similar substrates were placed on the top of each other, in the way that the areas of AC electrodes overlap each other. An example of component made by this design is illustrated in figure 21.

Figure 21. *The supercapacitor designed based on the second architecture.*

In the third architecture, a pre-coated copper substrate was used. After modification of the substrate, graphite ink was coated on the substrate and covered the entire surface. The modification of the copper substrate will be discussed in the next chapter. In this architecture copper, in combination with graphite, acts as the current collector. Figure 22 presents a schematic of a modified copper substrate before addition of graphene coating.

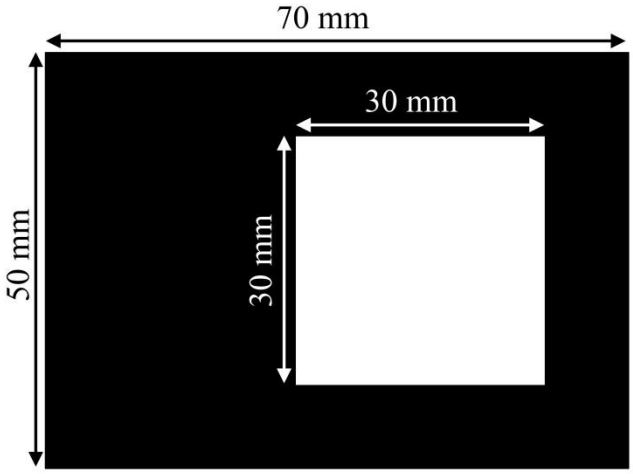

Figure 22. *The structure of a modified copper substrate.*

In this architecture, the electrode material with dimensions of 14*14 mm^2 must be coated onto the graphite surface and must be positioned in the center of the copper free area. A scheme of the substrate after coating of current collector and electrode can be seen in figure 23.

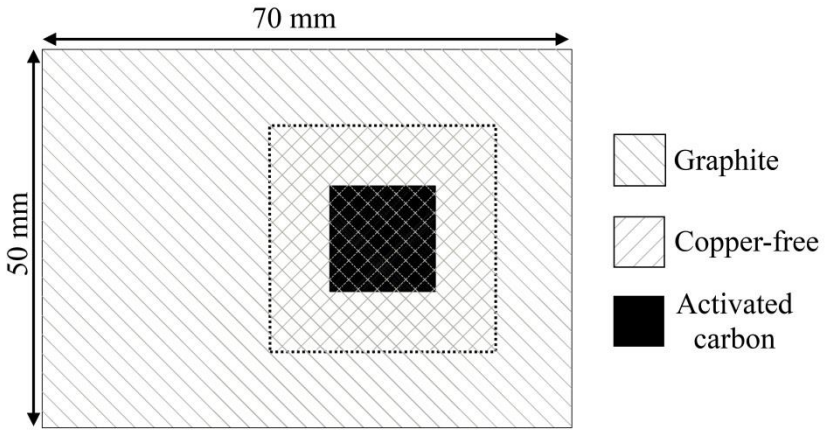

Figure 23. *The structure of a coated substrate with graphite (white) and electrode (black) on the top. Dotted area shows the copper free area on the substrate.*

In assembly, two similar substrates were placed on the top of each other, so that the areas of electrode coatings overlap each other. An example of a component made by this design is illustrated in figure 24.

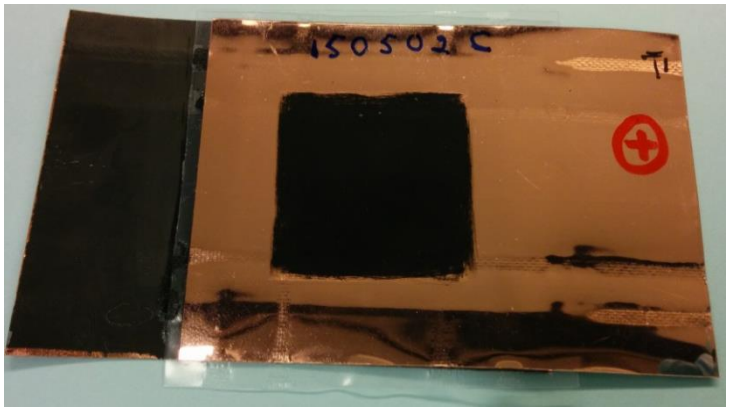

Figure 24. *The supercapacitor designed based on the third architecture.*

5.2.2 Etching

As mentioned earlier, corrosion of the current collectors decreases the life time of supercapacitors. In order to prevent corrosion, for a group of samples the active area on the copper substrate was etched before coating of electrodes. A layer of graphite was then coated over the entire substrate. Although there is no direct contact between the electrolyte and copper layer, without removing the copper below the electrode area the electrolyte might diffuse toward the substrate. Consequently, the electrolyte will be in contact with the copper layer and it could lead to the corrosion of this layer. Therefore, the idea was to remove the area of contact between ions and copper layer. An example of these samples is illustrated in figure 25.

The process of etching started with covering the copper substrate with a marker. The whole area of the sample has been covered by the marker, except the area which was desired to be etched. The function of the marker was to protect the copper substrate form being etched. Four different permanent markers were tested for this purpose, and only one of those had the complete protective functionality which was Artline 100. The etchant was prepared from the mixture of 30 mL hydrochloric acid (HCl), 30 mL hydrogen peroxide (H_2O_2), and 700 mL tap water. After etching for 1 minute the sample was exposed to the water in order to remove the acidic solution from surface. The final step was to clean the marker from the surface of the substrate using pure ethanol.

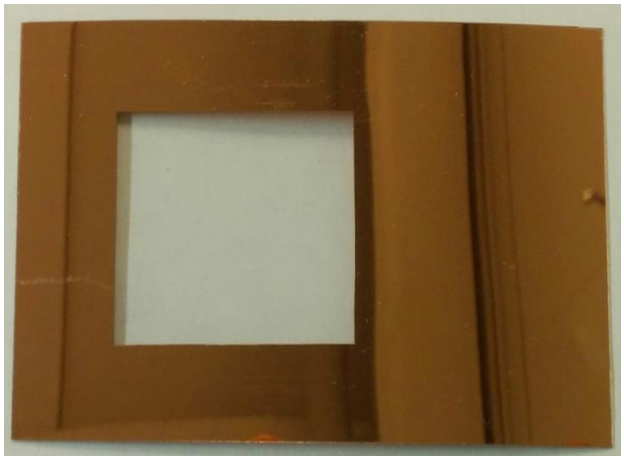

Figure 25. *Copper substrate after etching and cleaning.*

5.2.3 Coating

Based on the viscosity of the inks, blade coating was chosen as the deposition method. In this method, an applicator is moved across the substrate in order to distribute the ink. There are two main controllable parameters during coating: speed of the applicator and the desired wet thickness, set by the applicator. It must be considered that the coating thickness is also affected by the thickness of the covering mask of a substrate on which the applicator moves during the coating process. For all the prepared samples in this work, a covering mask with thickness of 65 µm was used. Moreover, the covering mask was connected to the substrate with a tape with thickness of 55 µm. The tape also applied on the covering mask, in a way that two sides of the applicator moves on the top of the tape. The target was an initial wet thickness of 120 µm, which is the combination of tape (55 µm) and mask (65 µm) thickness.

5.2.4 Surface modification

In some experiments, supercapacitors were made fabricated on the first architecture in order to test the behavior of the CNT ink alone to be used as the current collector and the electrode. The main challenge for these experiments was the poor adhesion of CNT

inks on the PET substrate. Therefore, surface modification of the PET surface was necessary. The modification was done by spreading a layer of Edolan on the PET surface. Coating of the Edolan was done using a spray gun. The drying of samples was done at 90°C for 30 minutes. An illustration of the modified surface can be seen in the figure 26. The area of modified surface was similar to the area of the electrode, which was 14*40 mm^2.

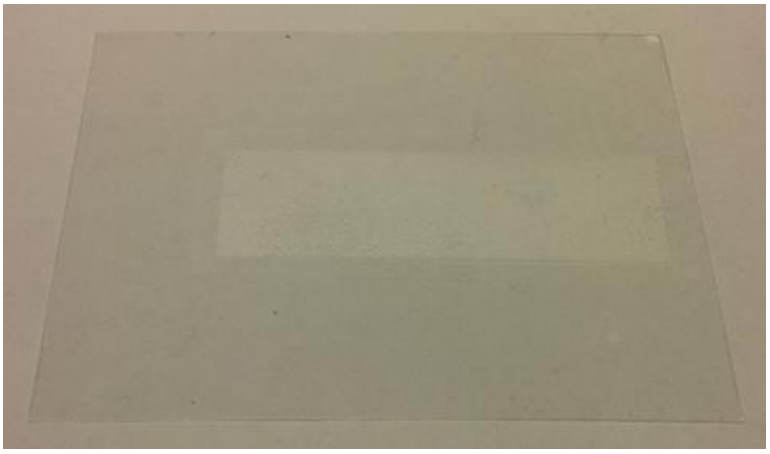

Figure 26. *PET substrate coated with Edolan (white area).*

5.2.5 Assembling and sealing

Assembling of supercapacitors was done in the ambient laboratory environment. The electrolyte was added to the active area of both electrodes, the separator was placed between two electrodes, and electrodes were placed on the top of each other so that the edges of active area of the two electrodes completely overlapped each other.

Sealing of supercapacitors has been done by two different approaches:

1. Applying of the adhesive tape on the substrate
2. Applying of sealing solution on the surface and sealing with hot sealing

In the first approach, NKK adhesive tape was used. The idea was to transfer the adhesive layer from the tape to the surface of the substrate. The size and design of the adhesive layer can be seen in figure 27. In order to have a more effective sealing, adhesive layer has been applied on both substrates.

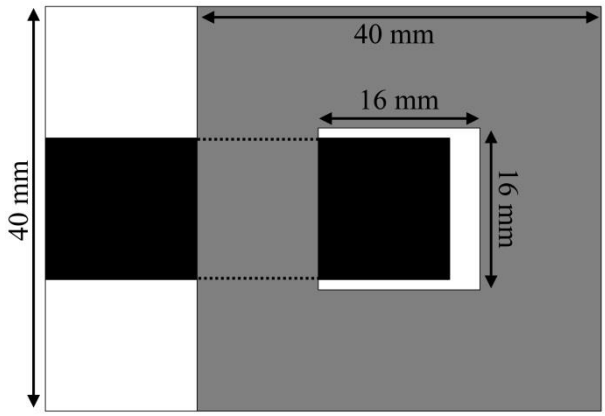

Figure 27. *Position of adhesive layer (gray) on the substrate. Black area represents printed current collector.*

Another approach for sealing was to use adhesive solution on the surface of substrates, followed by hot sealing of the component. For this purpose, X2277 sealing solution was used. After addition of the solution to the surface, it was dried at 80℃ for 30 minutes. In this sealing method, in order to protect the component from short circuit, there is a need for another layer between two plates of supercapacitor. The intermediate layer was Polyethylene (PE). This layer was designed in a way that it covers the whole area of contact between two substrates, except the electrode. It must be considered that this method was designed for the graphite coated copper substrates, and the functionality of the adhesive layer was not tested for PET substrate. The assembling was done in the following order:

1. Applying the sealing solution on both electrodes, followed by drying
2. Applying the PE layer on one electrode, and hot sealing with low temperature
3. Addition of electrolyte to the electrodes
4. Addition of separator layer
5. Placement of two substrates on the top of each other, so that there is a complete overlap of electrodes
6. Heat sealing of the system

An important consideration in this sealing method is that the heat sealing must be done on the copper free area in order to keep the electrolyte in the copper-free area. Incomplete sealing results in the penetration of the electrolyte to the copper substrate, which causes the corrosion of the substrate. The proper sealing edges can be seen in figure 28.

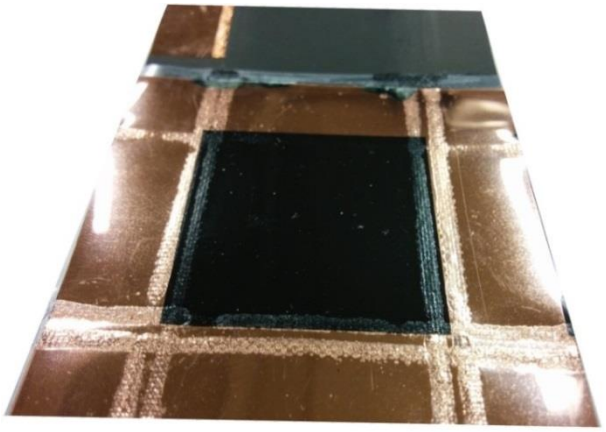

Figure 28. *A component with proper borders of sealing.*

5.3 Characterization

5.3.1 Electrical properties

The measured electrical properties for supercapacitors were sheet resistance, capacitance, leakage current, and ESR of component. Measurements were carried out using a Zennium electrochemical workstation from Zahner Elektrik GmbH. An illustration of this device can be seen in figure 29.

Figure 29. *Illustration of Zennium electrochemical workstation.*

For sheet resistance measurement, the device was set to a four-electrodes configuration, and it was connected to a four point probe. An illustration of the used configuration and probe can be seen in figure 30.

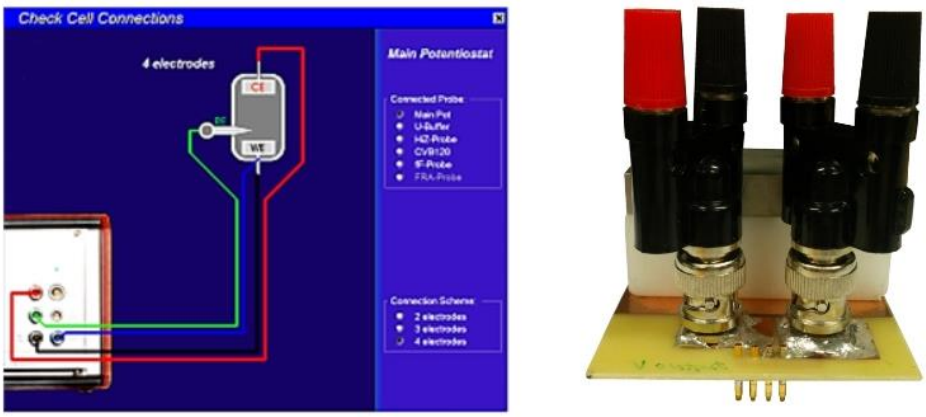

Figure 30. *Illustration of four-electrode configuration (left) and four-connection probe (right).*

The probe was placed on the middle, and in parallel with the length of printed layer. The sweep voltage of -200 to 200 mV was used in this measurement. Based on the geometry of dried samples, geometry correction factor of G = 0.73723 was used. Moreover, to increase the accuracy, each measurement was repeated three times for each sample and average value was calculated.

For cyclic voltammetry measurements, the device was set to a two-electrode configuration. The measurement was conducted in the voltage range of 0 to 0.9 V, and at different voltage sweep rates 100 mV/s, 50 mV/s, and 10 mV/s. At the next step, the component was cycled for twenty times at voltage sweep rate of 50 mV/s. Finally, samples were cycled with 100 mV/s and 50 mV/s.

Galvanostatic measurements were carried out based on IEC standard [15]. For galvanostatic measurements, an estimation of capacitance was obtained from cyclic voltammetry. From the obtained values of capacitance, a primary discharge current of component was calculated, and used in galvanostatic measurement. The maximum voltage of measurement was set to 0.9 V, and was conducted based on the explained procedure of the standard [15]. In the next step, measurement was repeated with the calculated values of discharge current from the previous step. Finally, the measurement was repeated with discharge current ten times bigger than the current used in the first measurement. The capacitance values of the component were recorded for each measurement.

The IR drop value of each component was obtained from the galvanostatic measurement with the highest current. The process for evaluation of leakage current was explained in section 4.2.

The last measurement for each component was cyclic voltammetry at sweep rate of 50 mV/s, and for 2000 cycles. The purpose of this measurement was to investigate the behavior of components during continuous cycling.

5.3.2 Surface and pore distribution

The importance of the surface area and pore size of the electrode has been explained earlier in this report. There are different methods for the measurement of surface area, but the best known is the Brunauer, Emmett, and Teller (BET) method [12]. This method is based on Langmuir theory and can be applied to monolayer and multilayer molecular adsorption. In the BET method, the surface area of solid material can be obtained by the physical adsorption of nitrogen gas molecules [43].

In order to investigate the pore structure and surface area of AC and graphene electrodes, BET analysis at 77 K was carried out. For this measurement, previously printed and dried samples were scratched from the surface of electrodes. In order to increase the accuracy of BET measurement, scratched powders were dried at 100°C for one hour.

6. RESULTS AND DISCUSSION

6.1 Coating and preparation of electrodes

As mentioned earlier, the coating of sample was done by blade coating on PET substrate and graphite. In case of CNT inks, adhesion to the substrate for both PET and graphite was poor. For PET substrate, the adhesion of ink tested after addition of a thin layer of Edolan. Surface modification of PET substrate with Edolan improved the adhesion of all Morphona CNT inks except NT20/S8010, BT50/S8020, BT50L20, and NC30S8015 inks. However, the film qualities were not satisfactory, and in many samples poor local adhesion of inks was visible after drying, as it can be seen in figure 31. The source of poor local adhesion was the agglomeration of CNT inks. For Bristol CNT ink, the poor wetting of ink made the process of coating impossible. Therefore, electrodes were prepared from step by step drying of individual drops on the substrate.

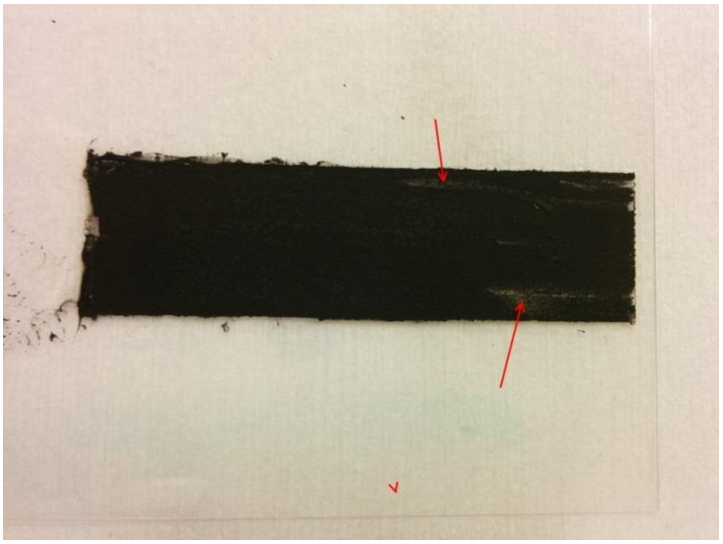

Figure 31. *Poor adhesion of CNT ink to PET substrate.*

In case of activated carbon and graphene inks, films were coated with a homogeneous thickness of 30 and 10 µm, respectively. The adhesion of inks to PET substrate and graphite layer was satisfactory. However, the main problem with graphene film was the drying procedure. Based on the datasheet, the drying of the ink must be done at 120°C for 2-4 minutes. However, inks dried based on the datasheet exhibited a flaky surface with visible cracks, as can be seen in figure 32.

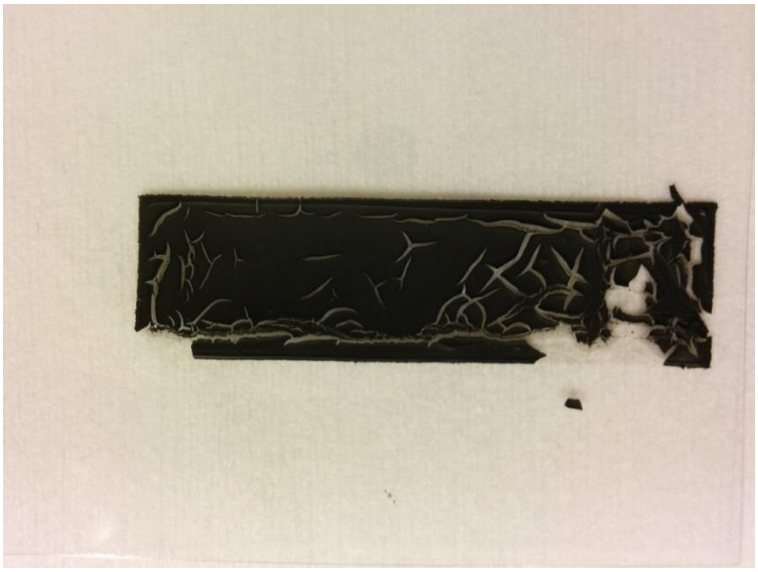

Figure 32. *Illustration of cracked surface of graphene ink after drying.*

Therefore, the drying condition was changed to 90°C for 30 minutes. Films dried at this condition had a suitable appearance with a homogenous thickness.

6.2 Electrochemical characterization

6.2.1 Sheet resistance

The values of R_S for CNT printed samples can be seen in figure 33. These values are for the samples made using the first architecture, in which current collector and electrode were made from the same ink. Compared to R_S values of graphene ink printed based on the same setup (4.5-11 Ω/sq), CNTs had higher R_S. Because of the low theoretical resistivity of CNTs and similar thickness ranges for graphene and CNT films (10-20 μm), high R_S values of CNTs were unexpected. One possible explanation is the low concentration of CNT inks, which was in the order of 1% to 5% of ink solution. Therefore, the printed network of CNTs may consist of isolated tubes which causes increased resistivity of the film and consequently sheet resistance values. Moreover, as stated in section 3.3 the length of CNTs play an important role in the conductivity of the printed samples. Short tubes lead to decreased connectivity of tubes in the network of the printed structure and consequently decreased conductivity.

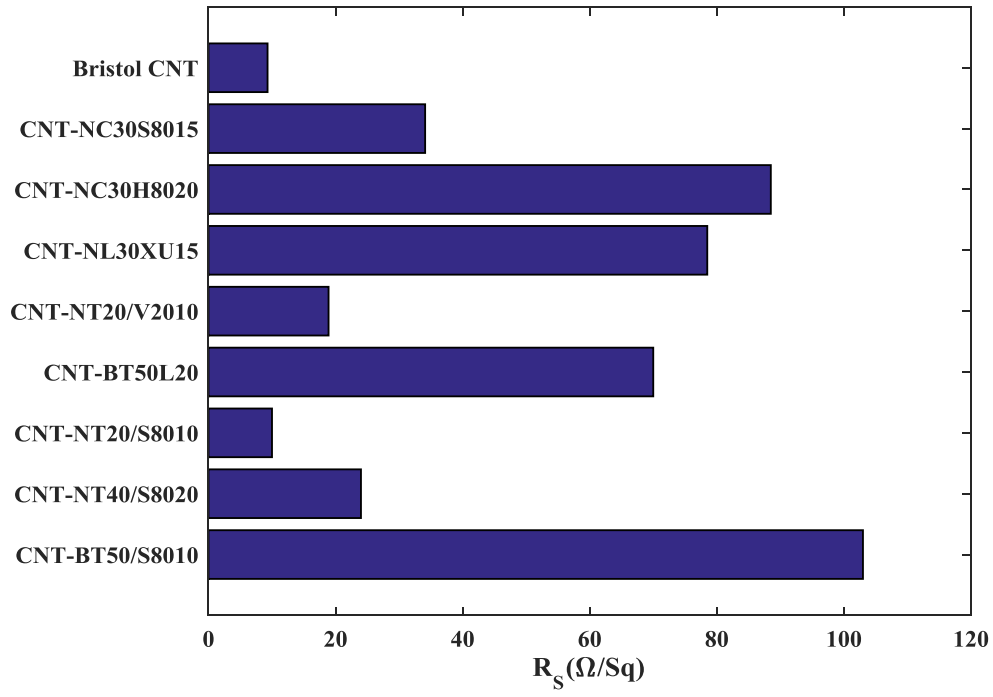

Figure 33. *Sheet resistance values of CNT samples.*

Based on the capacitance values of CNT inks, the sample with highest capacitance value was selected to be studied as the electrode material in other mask setups. A comparison of sheet resistance values of NT40/S8020 ink in different architectures of supercapacitors can be seen in figure 34.

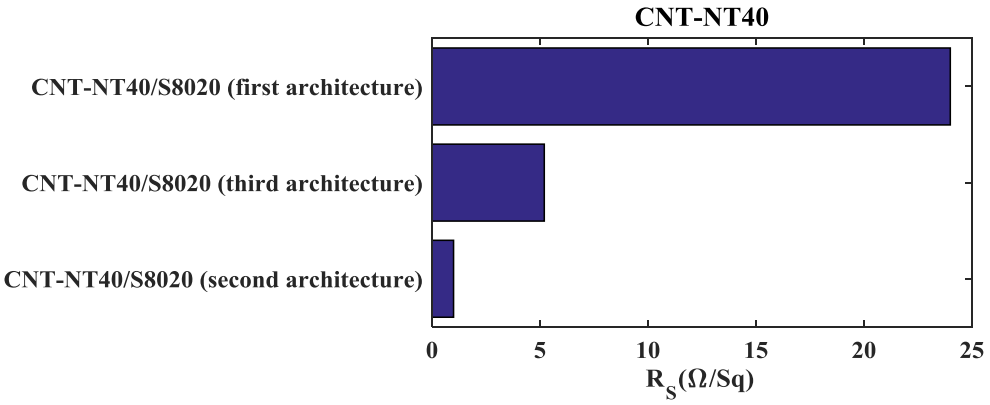

Figure 34. *Comparison of sheet resistance value of NT40/S8020 ink in different architectures.*

In figure 34, the first architecture refers to supercapacitors with CNT as current collector and electrode, the second architecture refers to components with silver and graphite as current collector, and the third architecture refers to samples with copper and graphite as current collector. As it can be seen, the use of conductive metals as current collector decreased sheet resistance values of CNT-based supercapacitors. Furthermore, silver

current collectors exhibit a better reduction of sheet resistance than copper current collectors.

6.2.2 Cyclic voltammetry

In order to investigate the behavior of supercapacitors, CV measurements of components were conducted. Figure 35, represents CV diagrams of CNT-NT40/S8020 at different sweeping rates of 100 mV/s, 50 mV/s, and 10 mV/s. The diagram presented on top is related to the sample made based on the third architecture (copper current collectors), and diagram on the bottom presents the sample made based on the first architecture with CNT as the electrode and current collector. In both samples, the CV behavior is relatively close to rectangular behavior of ideal supercapacitors. However, for the samples with copper current collectors (top) the CV behavior is more similar to that of the ideal supercapacitors.

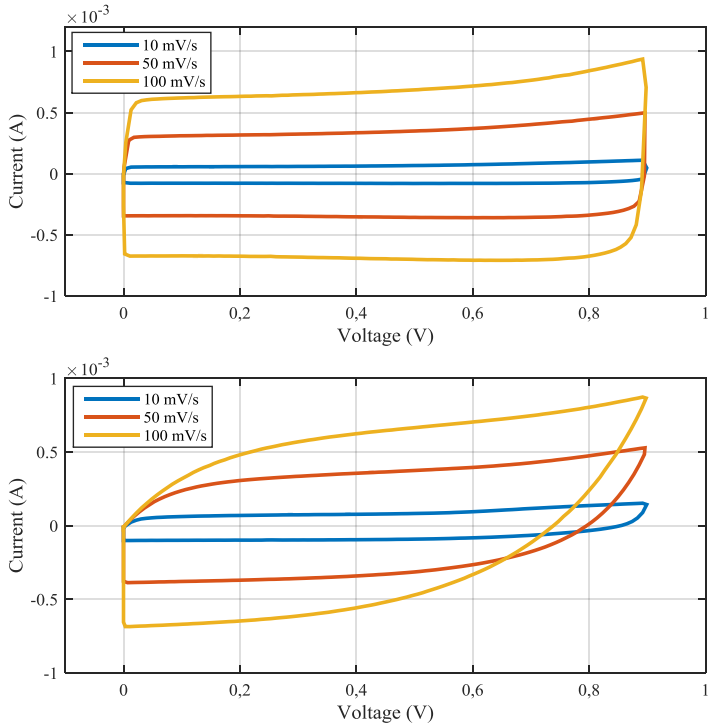

Figure 35. *CV diagram at voltage sweep rates of 100mv/s, 50 mV/s, and 10 mV/s for samples with copper current collector (top) and sample with CNT as current collector and electrode (bottom).*

The rectangular behavior of copper based samples is an indication of decreased values of resistance in the component.

Figure 36 shows the cyclic voltammetry diagrams of different samples at the voltage sweep rate of 10 mV/s. The rectangular behavior of supercapacitors for all the samples is visible. The top curve is a comparison of CV behavior of activated carbon in supercapacitors, which were designed based on the second architecture (with silver) and the

third architecture (with copper). The curve in the middle is the behavior of CNT ink in the same architectures, and the last curve presents the CV behavior of graphene designed with the first architecture.

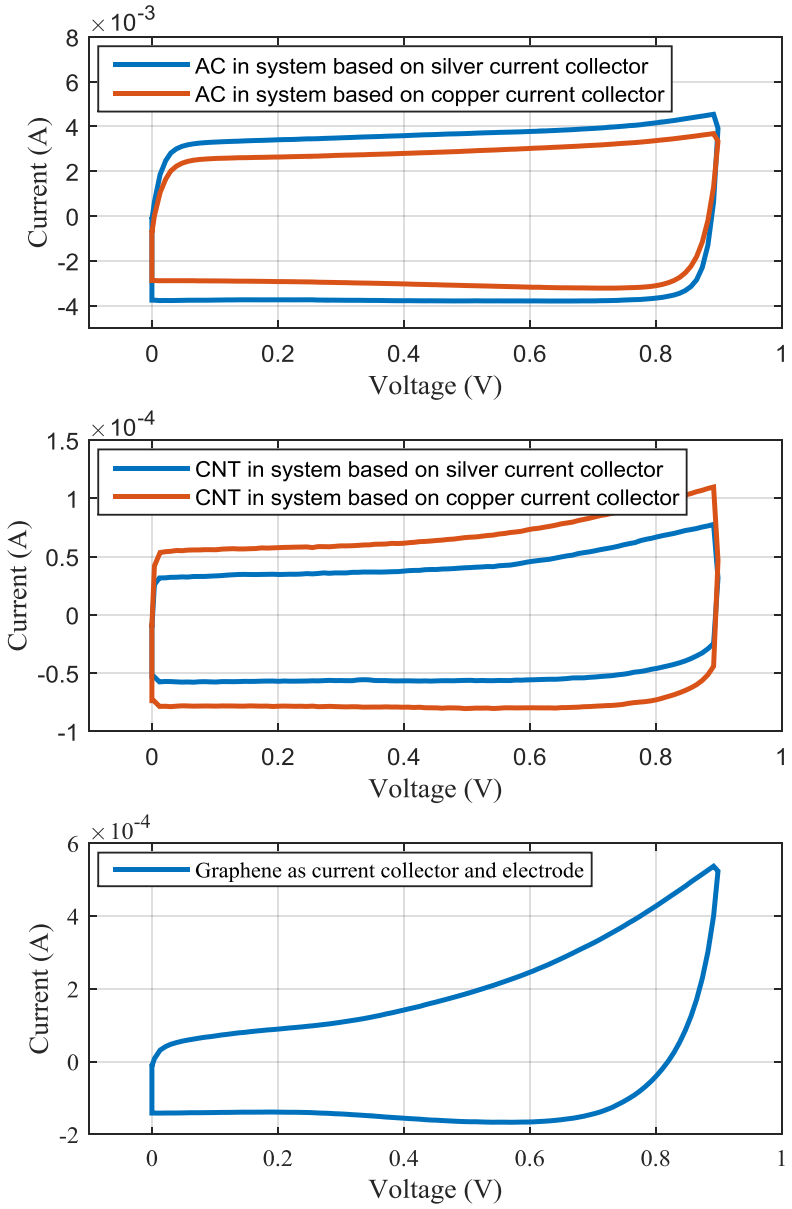

Figure 36. *CV curves of AC (top), CNT (middle), and graphene (bottom).*

For all the tested inks, the CV is relatively rectangular, with no peaks related to redox reactions. Therefore, in all the tested inks the capacitance mechanism is based on formation of double layers on electrodes. In all the samples, current increases at the high end of potential range, which is due to the leakage current at high voltage.

6.2.3 Capacitance values

A comparison of specific capacitance values of assembled supercapacitors obtained from galvanostatic measurements is shown in table 7. As explained in chapter 3, the specific capacitance of individual electrodes is four times bigger than that of the supercapacitor. The reported specific capacitance in this work is based on the masses of both electrodes.

Table 7. *Range of specific capacitance for assembled supercapacitors*

Electrode material	Material's code	Ranges of specific capacitance (F/g)
CNT	NT40/S8020	1.2 - 5.2
CNT	Except NT40/S8020	0.4 – 2.4
Graphene	N/A	1.8 – 7.1
Activated Carbon	N/A	17.7 – 33.3

The highest capacitance values are obtained from the samples with activated carbon electrodes. The high capacitance for activated carbon is an indication of high accessible surface area of the sample. As the values of capacitance for all CNT inks (except NT40/S8020) were close to each other, not all individual values are reported here. The wide range of specific capacitance of samples with the same electrode may be the result of misalignment between two active layers of a component. In case of CNT inks, the highest capacitance values obtained from CNT ink of NT40/S8020 with the highest specific capacitance of 5.2 F/g. For other CNT inks the highest values of 2.5 F/g was obtained. Based on the reported values of capacitance for the MWNTs (section 3.3), the CNT-based supercapacitors in this work exhibit smaller values than those reported in the literature. However, the capacitance of CNT-based supercapacitors mainly depends on the preparation method of electrodes. Based on the information stated in section 3.3, a great variety of parameters might be responsible for the small capacitance values of tested inks, namely blockage of surface area by binder materials, low accessible surface of CNT (because of low concentration of ink, or small lengths of CNTs, or agglomeration of CNTs), and random arrangement of CNTs in the structure of printed film. In order to correlate the small values of capacitance in CNT inks to the affecting factors, more detailed measurements are needed. For example, IR spectroscopy method is useful to study the blockage of surface by possible residual polymers and functional groups, and combination of transmission electron microscopy (TEM) and Raman spectroscopy methods are useful to study the structure and arrangement of CNTs.

6.2.4 ESR and leakage current

The ESR and leakage currents of different components are shown in table 8. As expected, ESR values of same electrode material are altered depending on the design architecture of component. In other words, use of highly conductive current collectors was beneficial in reducing the ESR values of supercapacitors. For example, CNT samples of BT50/8010 and NC30H8020 have ESR values of 850 and 500 Ω, respectively when they are used both as electrode and current collectors. However, when they were printed on graphite and copper current collectors, ESR decreased to 10 Ω for BT50/S8010 ink and 20 Ω for the NC30H8020 ink.

Table 8. *ESR and leakage current values of assembled supercapacitors*

Electrode material	Material's code	ESR (Ω)	Leakage current (μA)
CNTs designed with the first architecture	All	160 – 1140	0.1 – 5.9
	BT50/8010	850	3
	NC30H8020	500	0.1
CNT designed with the third architecture	All	6 – 20	0.1 - 5
	BT50/8010	10	3
	NC30H8020	20	3.8
Graphene designed with the first architecture	N/A	105 - 160	20 - 80
Activated carbon designed with the second architecture	N/A	2.5 – 13.7	8.3 – 13.7
Activated carbon designed with the third architecture	N/A	3.2 – 12.7	1 - 8

The highest ESR values were related to CNT samples designed with the first architecture, where CNT works as electrode and current collector. The ESR of supercapacitors with activated carbon electrodes was the lowest when deposited onto substrates using the third architecture (copper current collectors). In this work, the number of samples which were made based on silver current collector (second architecture) was limited. Therefore, the comparison between effectiveness of copper and silver current collectors in the reduction of ESR is not possible. Among different tested materials, CNTs exhibit the lowest leakage current, while the highest values were measured from graphene based supercapacitors. There was not any correlation between the design architecture of component and measured leakage current values.

6.3 BET analysis

In order to study the surface area of graphene and activated carbon electrodes BET analysis measurement was used. Based on this measurement, the specific surface area values of activated carbon and graphene was 1741 m^2/g and 5.5 m^2/g, respectively. The data obtained from BET measurement of activated carbon explains the high capacitance. On the other hand, the SSA value obtained from BET measurements of the graphene sample is surprisingly low. One possible explanation for low SSA values of the used graphene is the composition of ink. Based on a patent from the supplier [64], the ink appears to be not composed of pure graphene, but based on a mixture of polymeric binder, graphene, and graphite. Although they did not report an exact value for the SSA of ink, it was mentioned that the smallest SSA of this mixture is 100 m^2/g, depending on the composition of inks, which contradicts the results of this work. Figure 37 represents the pore size distribution of activated carbon ink from the BET measurement. As was expected, activated carbon has a porous structure with high concentration of mesopores. The average pore size distribution in activated carbon was in the range of 2 to 3 nm.

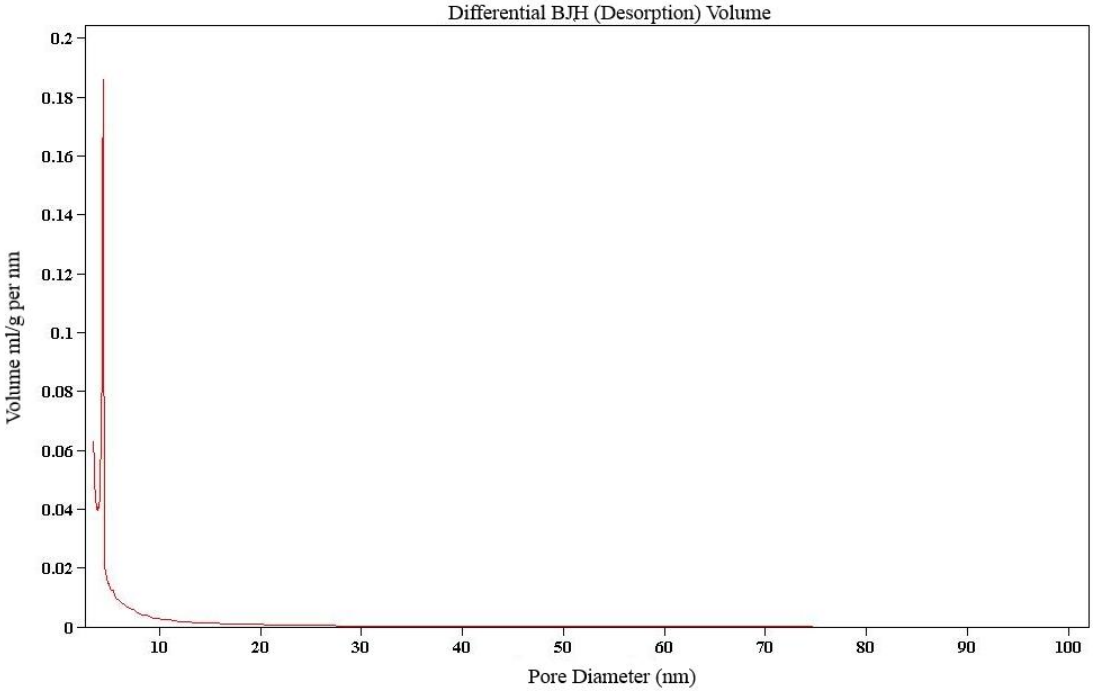

Figure 37. *Pore size distribution of activated carbon in mesopore range.*

As shown in figure 38, the main volume of pores in graphene had the same size distribution of 2 to 3 nm, In addition to pores with average sizes of 10 to 50 nm.

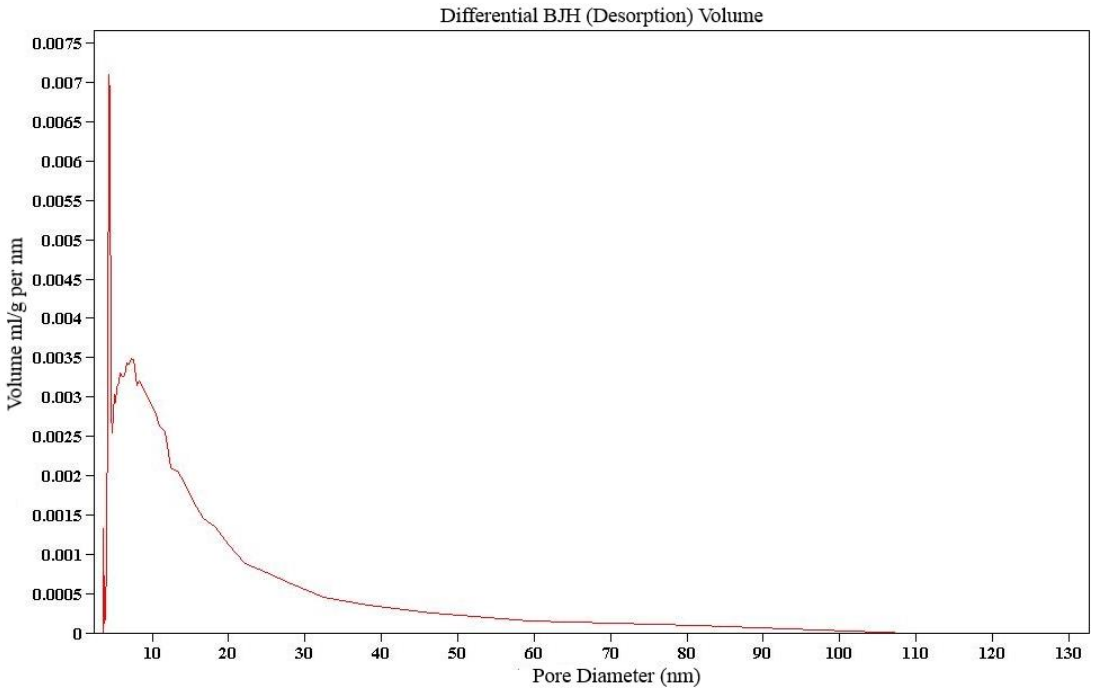

Figure 38. *Pore size distribution of graphene in mesopores range.*

6.4 Sealing efficiency

As mention in section 2.2.1, one disadvantage of aqueous supercapacitors is the corrosion of current collectors. Another criterion for comparison of success in different designs of supercapacitors was the corrosion of current collectors in each system. As stated in section 5.2.1, in samples which were designed based on the second architecture a combination of graphite and silver was used as the current collector. In all the samples designed based on this architecture, corrosion spots appeared on the surface of silver current collectors after two weeks storage of components. Figure 39 presents the appearance of the supercapacitor after corrosion (39.1), and optical microscopy image of corrosion spot on silver current collector (39.2). Therefore, the coverage of silver layer with graphite was not sufficient for the protection of silver from corrosion. Moreover, not only corrosion spots appeared in the active area (39.1.b), but also outside this area (39.1.a). It suggests that the sealing method in this model was not completely successful in maintaining the electrolyte in the mentioned area.

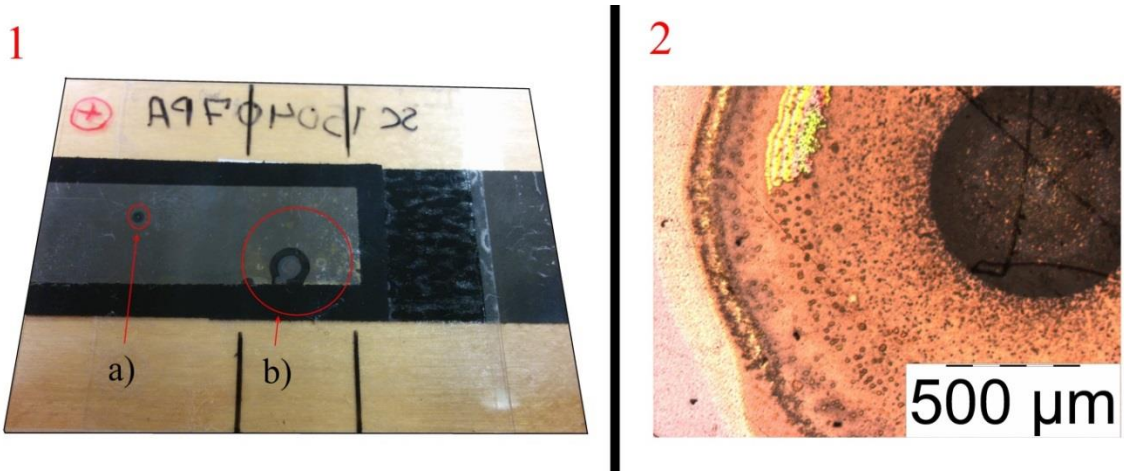

Figure 39. *Corrosion spots on silver current collector (1) and optical microscopy image of corrosion spot (2).*

Samples which used copper current collector showed no sign of corrosion, even after long time storage of components. Therefore, the third architecture design was successful in protection of copper current collector from corrosion.

7. CONCLUSION

In this work a variety of carbon-based inks were tested as the printed electrode of supercapacitors. The focus of work was to characterize the electrical properties of carbon-based electrodes. As the idea of work was to prepare environmentally friendly and flexible components, all the components made based on the use of aqueous electrolyte. Therefore, the aim was to design components with suitable performance without the potential disadvantage of aqueous electrolyte in the corrosion of current collectors.

In terms of printability, CNT inks did not exhibit a suitable adhesion. Further modification of the substrate also did not improve the adhesion of inks to the substrate. Coupled with the presence of agglomerates in the solution of these inks, CNTs did not exhibit suitable printability. In addition, these inks did not exhibit good electrical performances as their sheet resistance was in the range of 9.3 to 103 Ω/sq for average electrode thickness of 15 μm. In light of the average small specific capacitance of 2 F/g for these inks, it can be concluded that current inks are not suitable for use as supercapacitor electrodes, and further development of CNT inks is necessary for their implementation in supercapacitor applications.

On the other hand, electrodes which were prepared with AC inks exhibited high specific capacitance of 33 F/g. BET analysis of AC powder showed high specific surface area of 1741 m^2/g, which suggests that the printed AC ink has a high concentration of pores, and is suitable for preparation of printable supercapacitors. In case of graphene inks, the value of SSA was 5.5 m^2/g which is smaller than predicted values from the provider [64]. However, the capacitance of the sample with the highest values of 7.1 F/g was not in agreement with the results of BET analysis.

It has been shown that the electrical performance of supercapacitors can be increased significantly, by the use of modified copper-coated substrates. Aside from the type of tested carbon-based inks, the sheet resistance and ESR of the printed supercapacitors were decreased significantly in systems with the modified copper current collectors, and without deterioration of components quality. In this work, the best supercapacitors were achieved for AC-based supercapacitors which were printed on copper current collector with high specific capacitance values of 33 F/g and ESR smaller than 12.7 Ω.

Bibliography

[1] Lu, Max. Beguin, Farncois. Frackowiak E. Supercapacitors : Materials, Systems and Applications. 1st ed. Wiley; 2013. 569 p.

[2] Chen T, Dai L. Carbon nanomaterials for high-performance supercapacitors. Mater Today [Internet]. 2013 Jul;16(7-8):272–80. Available from: http://linkinghub.elsevier.com/retrieve/pii/S136970211300223X

[3] Gao Q. Optimizing carbon / carbon supercapacitors in aqueous and organic electrolytes. PhD Thesis, Univ Orleans [Internet]. 2013; Available from: http://tel.archives-ouvertes.fr/docs/00/87/20/80/PDF/qiang.gao_3317.pdf

[4] Leenen MAM, Arning V, Thiem H, Steiger J, Anselmann R. Printable electronics: flexibility for the future. Phys status solidi [Internet]. 2009 Apr;206(4):588–97. Available from: http://doi.wiley.com/10.1002/pssa.200824428

[5] Kaempgen M, Chan CK, Ma J, Cui Y, Gruner G. Printable Thin Film Supercapacitors Using Single-Walled Carbon Nanotubes. Nano Lett [Internet]. 2009 May 13;9(5):1872–6. Available from: http://pubs.acs.org/doi/abs/10.1021/nl8038579

[6] Faculty TA, Zhou C, Fulfillment IP, Engineering F. Carbon Nanotube Based Electrochemical Supercapacitors. 2006;

[7] Li ZL. Carbon-Based Materials As Supercapacitor Electrodes Carbon-Based Materials As Supercapacitor Electrodes. 2010;

[8] An KH, Kim WS, Park YS, Moon JM, Bae DJ, Lim SC, et al. Electrochemical properties of high-power supercapacitors using single-walled carbon nanotube electrodes. Adv Funtional Mater. 2001;11(5):387–92.

[9] Kötz R, Carlen M. Principles and applications of electrochemical capacitors. Electrochim Acta. 2000;45(15-16):2483–98.

[10] Yu G, Xie X, Pan L, Bao Z, Cui Y. Hybrid nanostructured materials for high-performance electrochemical capacitors. Nano Energy [Internet]. Elsevier; 2013;2(2):213–34. Available from: http://dx.doi.org/10.1016/j.nanoen.2012.10.006

[11] Du C, Pan N. Carbon Nanotube-Based Supercapacitors. 2007;569–76.

[12] Conway BE. Electrochemical Supercapacitors: Scientific Fundamentals and Technological Applications. Plenum Publishers; 1999.

[13] Youssef Diab, Pascal Venet, Hamid Gualous G´R. Self-Discharge Characterization and Modeling of Electrochemical Capacitor Used for Power Electronics Applications. Inst Electr Electron Eng. 2009;24 (2):510–7.

[14] Niu J, Conway BE, Pell WG. Comparative studies of self-discharge by potential decay and float-current measurements at C double-layer capacitor and battery electrodes. J Power Sources [Internet]. 2004;135(1-2):332–43. Available from: http://www.sciencedirect.com/science/article/pii/S0378775304004860

[15] International Electrochemical Commission. International Standard: Fixed electric double-layer capacitors for use in electronic equipment. First. IEC 62391-1.

[16] Ayadi M. Voltage and Temperature Impacts on Leakage current in calendar Agening of Supercapacitors. In: Power Engineering, Energy, and Electrical devices. Istanbul; 2013. p. 1466–70.

[17] Su Y. Advanced Electrode Materials for Electrochemical Supercapacitors. Access. 2015.

[18] Snook G a., Kao P, Best AS. Conducting-polymer-based supercapacitor devices and electrodes. J Power Sources [Internet]. Elsevier B.V.; 2011;196(1):1–12. Available from: http://dx.doi.org/10.1016/j.jpowsour.2010.06.084

[19] Chen S, Ramachandran R, Mani V, Saraswathi R. Recent Advancements in Electrode Materials for the High- performance Electrochemical Supercapacitors : A Review. 2014;9:4072–85.

[20] Qu D, Qu D, Shi H, Shi H. Studies of activated carbons used in double-layer capacitors. Construction. 1998;99–107.

[21] Jampani P, Manivannan a., Kumta PN. Advancing the Supercapacitor Materials and Technology Frontier for Improving Power Quality. Electrochem Soc Interface [Internet]. 2010;19(3):57–62. Available from: https://www.electrochem.org/dl/interface/fal/fal10/fal10_p057-062.pdf

[22] Miyake M. Electrochemical Functions. In: Carbon Alloys: Novel Concepts to Develop Carbon Science and Technology. Elsevier B.V.; 2003.

[23] Frackowiak, E., Beguin FF. Carbon Materials for the Electrochemical Storage of Energy in apacitors. Carbon N Y. 2001;39:937–50.

[24] Yang H. Graphene-based Supercapacitors for Energy Storage Applications. The Ohio State University; 2013.

[25] Pan H, Li J, Feng YP. Carbon nanotubes for supercapacitor. Nanoscale Res Lett. 2010;5(3):654–68.

[26] Barbieri O, Hahn M, Herzog A, Kötz R. Capacitance limits of high surface area activated carbons for double layer capacitors. Carbon N Y [Internet]. 2005 May;43(6):1303–10. Available from: http://linkinghub.elsevier.com/retrieve/pii/S0008622305000047

[27] Le LT, Ervin MH, Qiu H, Fuchs BE, Lee WY. Graphene supercapacitor electrodes fabricated by inkjet printing and thermal reduction of graphene oxide. Electrochem commun [Internet]. 2011 Apr;13(4):355–8. Available from: http://linkinghub.elsevier.com/retrieve/pii/S1388248111000361

[28] Gyoung-Ja L. Synthesis and Characterization of Nanoporous Carbon and Its Electrochemical Application to Electrode Material for Supercapacitors. In: Vayenas CG (Ed. ., editor. Modern Aspects of Electrochemistry 41. Newyork: Springer; 2007.

[29] Alwarappan, Subbiah. Kumar A. Graphene-Based Materials: Science and Applications. CRC Press; 2013. 224 p.

[30] Bachmatiuk WSR. Graphene: Fundamentals and emergent applications. 2013. 470 p.

[31] Scenev V. Electronic properties of graphene and other carbon-based hybrid materials for flexible electronics. Humboldt University of Berlin; 2014.

[32] Wang Y, Shi Z, Huang Y, Ma Y, Wang C, Chen M, et al. Supercapacitor Devices Based on Graphene Materials. J Phys Chem C [Internet]. 2009 Jul 30;113(30):13103–7. Available from: http://pubs.acs.org/doi/abs/10.1021/jp902214f

[33] Liu C, Yu Z, Neff D, Zhamu A, Jang BZ. Graphene-Based Supercapacitor with an Ultrahigh Energy Density. Nano Lett [Internet]. 2010 Dec 8;10(12):4863–8. Available from: http://pubs.acs.org/doi/abs/10.1021/nl102661q

[34] Quintana M, Tapia JI, Prato M. Liquid-phase exfoliated graphene: functionalization, characterization, and applications. Beilstein J Nanotechnol [Internet]. 2014 Dec 4;5:2328–38. Available from: http://www.beilstein-journals.org/bjnano/content/5/1/242

[35] Yuan W, Zhou Y, Li Y, Li C, Peng H, Zhang J, et al. The edge- and basal-plane-specific electrochemistry of a single-layer graphene sheet. Sci Rep [Internet]. 2013 Jul 30;3. Available from: http://www.nature.com/articles/srep02248

[36] S R C VIVEKCHAND, CHANDRA SEKHAR ROUT. Graphene-based electrochemical supercapacitors. J Chem Sci. 2008;120, 1:9–13.

[37] Korkut S, Roy-Mayhew JD, Dabbs DM, Milius DL, Aksay IA. High Surface Area Tapes Produced with Functionalized Graphene. ACS Nano [Internet]. 2011 Jun 28;5(6):5214–22. Available from: http://pubs.acs.org/doi/abs/10.1021/nn2013723

[38] Cao X, Yin Z, Zhang H. Three-dimensional graphene materials: preparation, structures and application in supercapacitors. Energy Environ Sci [Internet]. 2014 Feb 24;7(6):1850–65. Available from: http://xlink.rsc.org/?DOI=C4EE00050A

[39] Fan Z, Yan J, Zhi L, Zhang Q, Wei T, Feng J, et al. A Three-Dimensional Carbon Nanotube/Graphene Sandwich and Its Application as Electrode in Supercapacitors. Adv Mater [Internet]. 2010 Sep 1;22(33):3723–8. Available from: http://doi.wiley.com/10.1002/adma.201001029

[40] Qu D. Studies of the activated carbons used in double-layer supercapacitors. J Power Sources. 2002;109:403–11.

[41] El-Kady MF, Strong V, Dubin S, Kaner RB. Laser Scribing of High-Performance and Flexible Graphene-Based Electrochemical Capacitors. Science (80-) [Internet]. 2012 Mar 16;335(6074):1326–30. Available from: http://www.sciencemag.org/cgi/doi/10.1126/science.1216022

[42] B. Viswanathan PIN and TKV. Methods of Activation and Specific Applications of Carbon Materials [Internet]. Chennai, India; 2009. Available from: https://nccr.iitm.ac.in/e book-Carbon Materials final.pdf

[43] Lee G, Pyun S. Synthesis and Characterization of Nanoporous Carbon and Its Electrochemical Application to Electrode Material for Supercapacitors. Most. 2007;(41):139–95.

[44] Mitsuhiro Nakamura, Masanori Nakanishi KY. Influence of physical properties of activated carbons on characteristics of electric double-layer capacitors. J Power Sources. 1996;60:225–31.

[45] V. Ruiz, C. Blanco, M. Granda RS. Enhanced life-cycle supercapacitors by thermal treatment of mesophase-derived activated carbons.

[46] Chunsheng D. Carbon Nanotube-Based Supercapacitors. Nanotechnol LAW Bus. 2007;4, No.1:569–76.

[47] Gebhardt B. Type Selective Functionalization of Single-Walled Carbon Nanotubes. University of Erlangen-Nuremberg; 2012.

[48] Taczak MD. Controlling the Structure and Properties of Carbon Nanotubes. Virginia; 2007.

[49] Prasek J, Drbohlavova J, Chomoucka J, Hubalek J, Jasek O, Adam V, et al. Methods for carbon nanotubes synthesis—review. J Mater Chem [Internet]. 2011;21(40):15872. Available from: http://xlink.rsc.org/?DOI=c1jm12254a

[50] Peigney A, Laurent C, Flahaut E, Bacsa RR, Rousset A. Specific surface area of carbon nanotubes and bundles of carbon nanotubes. Carbon N Y

[Internet]. 2001 Apr;39(4):507–14. Available from: http://linkinghub.elsevier.com/retrieve/pii/S000862230000155X

[51] Niu C, Sichel EK, Hoch R, Moy D, Tennent H. High power electrochemical capacitors based on carbon nanotube electrodes. Appl Phys Lett [Internet]. 1997;70(11):1480. Available from: http://scitation.aip.org/content/aip/journal/apl/70/11/10.1063/1.118568

[52] Shiraishi S. Electric Double Layer Capacitors. In: Carbon Alloys: Novel Concepts to Develop Carbon Science and Technolog. Gunma, Japan: Gulf Professional Publishing; 2003. p. 584.

[53] Frackowiak E, Jurewicz K, Szostak K, Delpeux S, Béguin F. Nanotubular materials as electrodes for supercapacitors. Fuel Process Technol [Internet]. 2002 Jun;77-78:213–9. Available from: http://linkinghub.elsevier.com/retrieve/pii/S0378382002000784

[54] Lu W, Qu L, Henry K, Dai L. High performance electrochemical capacitors from aligned carbon nanotube electrodes and ionic liquid electrolytes. J Power Sources [Internet]. 2009 Apr;189(2):1270–7. Available from: http://linkinghub.elsevier.com/retrieve/pii/S0378775309000500

[55] Guo SR, Wang W, Ozkan CS, Ozkan M. Assembled graphene oxide and single-walled carbon nanotube ink for stable supercapacitors. J Mater Res [Internet]. 2013;28(7):918–26. Available from: <Go to ISI>://000316917100003

[56] Jiang L, Gao L, Sun J. Production of aqueous colloidal dispersions of carbon nanotubes. J Colloid Interface Sci [Internet]. 2003 Apr;260(1):89–94. Available from: http://linkinghub.elsevier.com/retrieve/pii/S0021979702001765

[57] Tortorich R, Choi J-W. Inkjet Printing of Carbon Nanotubes. Nanomaterials [Internet]. 2013 Jul 29;3(3):453–68. Available from: http://www.mdpi.com/2079-4991/3/3/453/

[58] Lei C, Lekakou C. Carbon-based nanocomposite EDLC supercapacitors. Etc [Internet]. :0–4. Available from: http://epubs.surrey.ac.uk/713748/1/Carbon-based nanocomposite EDLC supercapacitors.doc

[59] Zanello P. Inorganic Electrochemistry: Theory, Practice and Application. The Royal Society of Chemistry; 2003.

[60] Simon P. Materials for Electrochemical Capacitors. Nat Mater. 2008;7:845–54.

[61] B.E. Conway WGP. Power limitations of supercapacitor operation associated with resistance and capacitance distribution in porous electrode devices. J Power Sources. 2002;105:169–81.

[62] Julin T. Flexo-printed piezoelectric PVDF pressure sensors. Tampere University of Technology; 2011.

[63] Smits FM. Measurement of Sheet Resistivities with the Four-Point Probe. Bell Syst Tech J [Internet]. 1958 May;37(3):711–8. Available from: http://ieeexplore.ieee.org/lpdocs/epic03/wrapper.htm?arnumber=6773368

[64] Vrma, Vipin. Scheffer, Dan. Ginneman, Carl. Lettow JS. POLYMERIC COMPOSITIONS CONTAINING GRAPHENE SHEETS AND GRAPHITE. USA; US 2012/0142832 A1, 2012. p. 11.